Journal of Materials Chemistry B

ROYAL SOCIETY OF CHEMISTRY

REVIEW

View Article Online
View Journal | View Issue

Cite this: J. Mater. Chem. B, 2023, 11, 8897

Intelligent sensing based on active micro/nanomotors

Lingfeng Jiang,[a] Xiaoxia Liu,[b] Dongfang Zhao,[b] Jinhong Guo,*[ac] Xing Ma *[b] and Yong Wang *[a]

Received 22nd May 2023,
Accepted 10th August 2023

DOI: 10.1039/d3tb01163a

rsc.li/materials-b

In the microscopic world, synthetic micro/nanomotors (MNMs) can convert a variety of energy sources into driving forces to help humans perform a number of complex tasks with greater ease and efficiency. These tiny machines have attracted tremendous attention in the field of drug delivery, minimally invasive surgery, *in vivo* sampling, and environmental management. By modifying their surface materials and functionalizing them with bioactive agents, these MNMs can also be transformed into dynamic micro/nano-biosensors that can detect biomolecules in real-time with high sensitivity. The extensive range of operations and uses combined with their minuscule size have opened up new avenues for tackling intricate analytical difficulties. Here, in this review, various driving methods are briefly introduced, followed by a focus on intelligent detection techniques based on MNMs. And we discuss the distinctive advantages, current issues, and challenges associated with MNM-based intelligent detection. It is believed that the future advancements of MNMs will greatly impact the diagnosis, treatment, and prevention of diseases.

1. Introduction

The rapid advancement in micro/nanotechnology and the continuous improvement of micro/nanostructure characterization and control methods have greatly facilitated the development and utilization of micro/nanoscale devices.[1,2] The high specific surface area and remarkable catalytic properties of various micro/nanomaterials have made them a popular choice in the construction of biosensors, leading to the development of biosensors with high specificity, high throughput, and high sensitivity.[3–5]

[a] *Key Laboratory of Clinical Laboratory Diagnostics (Ministry of Education), College of Laboratory Medicine, Chongqing Medical University, Chongqing 400016, China. E-mail: wangyong@cqmu.edu.cn, guojinhong@sjtu.edu.cn*
[b] *Sauvage Laboratory for Smart Materials, School of Materials Science and Engineering, Harbin Institute of Technology (Shenzhen), Shenzhen 518055, China. E-mail: maxing@hit.edu.cn*
[c] *School of Sensing Science and Engineering, Shanghai Jiao Tong University, Shanghai, China*

Lingfeng Jiang

Lingfeng Jiang received his BS degree in Laboratory technology from Chongqing Medical University, China, in July 2020. He is currently working toward a MS degree in Medical Technology with the School of Laboratory Medicine, Chongqing Medical University, China. His research interests include motion control of micro/nanomotors and their application in sensing detection.

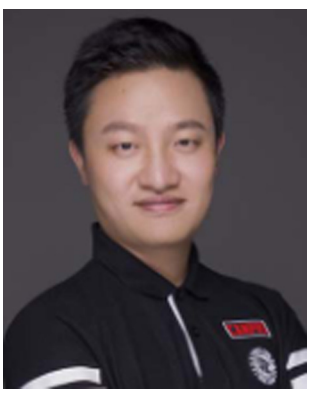

Jinhong Guo

Jinhong Guo received his PhD degree in biomedical engineering from Nanyang Technological University, Singapore, in 2014. Upon completing the doctoral program, he served as a Postdoctoral Fellow with the Pillar of Engineering Design, MIT-SUTD, Singapore, from 2014 to 2015. He is currently a Full Professor with Shanghai Jiao Tong University, Shanghai, China, and an Executive Dean of Chongqing Medical University, Chongqing, China. At present, his research revolves around the development of electrochemical sensors and lab-on-a-chip devices for point-of-care testing aimed at clinical applications.

However, these sensing systems mainly use micro/nanomaterials to construct trace probes and sensing interfaces, of little use as standalone nano-sensors. Furthermore, the lack of autonomous motion capability in most micro/nanomaterials restricts the progress of intelligent micro/nano-sensing.

Micro/nanomotors (MNMs) are a class of synthetic micro/nano scale machines that mimic the functions of natural mobile microorganisms.[6] These machines rely on the conversion of energy to produce autonomous movement in micro/nano environments.[7] These tiny motors can be powered by various sources, including chemical reactions,[8,9] ultrasound,[10] electrical fields,[11] light,[12,13] and magnetic fields.[14,15] MNMs are incredibly small, ranging in size from a few micrometers to a few hundred nanometers, and they can provide a direct, mechanical response to changes in the environment. As a result, they are highly suitable for target molecule detection in a wide range of environments. Additionally, their controllable motion mode and simple preparation process make them highly attractive for use in various fields, including environmental remediation,[16,17] drug delivery,[18,19] and minimally invasive surgery.[20] Especially, they have significant application value in the fields of developmental trends in the preparation of micro biosensors.[21–23] There are several features that recommend MNMs for sensing. First, the independent and continuous movement of MNMs enhanced micro-mixing of fluids, resulting in improved mass transfer and collisions between MNMs and targeted analytes. Simultaneously, MNMs can function as mobile reaction sites, broadening the range and enhancing the sample processing capacity through surface modification with reactive agents and groups. Furthermore, MNMs can be made small enough to access areas that are inaccessible to traditional sensors, such as inside the human body or in small-scale industrial processes.

In recent years, extensive research studies have been conducted to investigate sensing applications using MNMs. MNMs have been equipped with nanoscale sensors to detect changes in physical or chemical parameters actively, such as pH,[24] metal ions[25,26] or specific biomarkers.[27–29] By combining the sensing capabilities of these nanoscale sensors with the motion of the MNM, it is possible to create highly sensitive and responsive sensors that can provide real-time information about the environment. The prospects for the use of self-propelled MNMs in sensing appear to be bright. Up to now, although several remarkable reviews have addressed certain aforementioned topics, including the preparation and functionalization of MNMs,[30–33] driving modes,[34,35] biocompatibility of MNMs for sensing applications,[23] their sensing strategies and detecting substances,[22,36,37] these reviews mainly focus on MNM functionalization as well as sensing applications from a certain perspective. The key challenges and limitations of MNMs for sensing applications may not have been thoroughly explored. Building upon this foundation, the current review presents a concise overview of the most recent research in the realm of biosensors, specifically emphasizing the application and detection principles of MNMs. Furthermore, we emphasize the key advantages and challenges associated with the use of MNMs for practical sensing applications.

2. Propulsion mechanisms of MNMs

The American science fiction film *Fantastic Voyage* from the 1970s tells the story of five doctors who were shrunk to a few millionths and then injected into a patient's blood vessels to perform surgery. Since then, people began to conceive solving some bottleneck problems in the medical field by preparing micro/nano scale robots to enter the human body. In fact, there are many natural MNMs in nature. For example, by consuming adenosine triphosphate (ATP), the functional proteins in the cell can move along the microtubules in the cell and carry protein molecules at the micro/nano scale to ensure the normal operation of various functions in the cell and these functional proteins with the ability to move are natural micro/nanorobots.[38] *E. coli* can promote its own movement through flagellar movement to obtain food and avoid adverse factors.[39] Animal sperm cells can also bind to ova through flagellar motility combined with

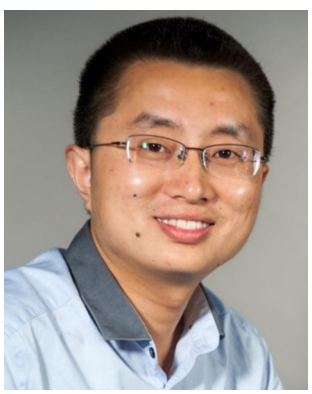

Xing Ma

Xing Ma obtained his PhD degree in materials science and engineering from Nanyang Technological University in 2013. He worked as an Alexander von Humboldt research fellow at the Max Planck Institute for Intelligent Systems (MPI-IS) in Germany, from 2014 to 2016. He is now a professor in Harbin Institute of Technology (Shenzhen), China. His research focuses on micro/nanomotors for biomedical applications and intelligent micro/nanodevices or biosensing.

Yong Wang

Yong Wang obtained his PhD degree in materials science and engineering from Harbin Institute of Technology (Shenzhen) in 2022. He is now an associate professor in Chongqing Medical University, China. The primary focus of his research lies in the application of micro/nanomotors in the field of in vitro detection.

their self-generated chemotactic properties.[40] Inspired by these natural biological robots, scientists have studied and designed micro-and nanostructures that can transform the energy of their surroundings to motion autonomously and achieve specific tasks, commonly referred to as MNMs. With the ability to move in a controlled manner at the micro/nano scale, MNMs have important applications in drug delivery,[41] minimally invasive surgery,[20] single cell manipulation,[6] environmental remediation[16] and biosensing,[22] opening up new minimally invasive and highly specific treatment methods for the medical field.

At the micro/nano scale, the Reynolds number decreases rapidly due to the dramatic reduction in size, viscous drag dominates and inertial forces are negligible. This leads to the fact that the propulsion methods and mechanisms of machines in the macroscopic world (with a high Reynolds number) are no longer applicable at the micro/nano scale. In the 1970s, Purcell gave a lecture on 'Life in a low Reynolds number environment', which led to a number of groundbreaking theories and initiated nearly half a century of research into the mechanisms of microbial swimming. The morphological processes of conch opening and closing are temporally symmetrical and do not produce a net movement if the conch opens and closes under low Reynolds number conditions. It has been shown that microorganisms need to break the temporal symmetry to swim in a low Reynolds number environment, which is often referred to as the scallop theorem. This is also a guideline for the design of different self-driven MNMs. The following is a brief description of the current main propulsion mechanisms of MNMs, which are broadly classified as chemical, external and biomass propulsion.

2.1 Internal chemically driven MNMs

(1) Bubble propulsion. The MNMs driven by bubbles can achieve spontaneous directional motion by breaking the symmetry of the bubble release direction. This is achieved by using a catalytic material loaded onto the micro/nano structure material to react with a substrate in solution (*e.g.* hydrogen peroxide) to produce bubbles, and the separation or bursting of the bubbles produces a recoil that drives the motor. Due to its good catalytic activity for decomposing H_2O_2, the noble metal platinum (Pt) has become the most widely used inorganic catalyst for the preparation of MNMs in various structures[42,43] (Fig. 1a). Considering the scarcity and high cost of Pt, researchers have also used other chemical reactions to replace Pt catalysts for

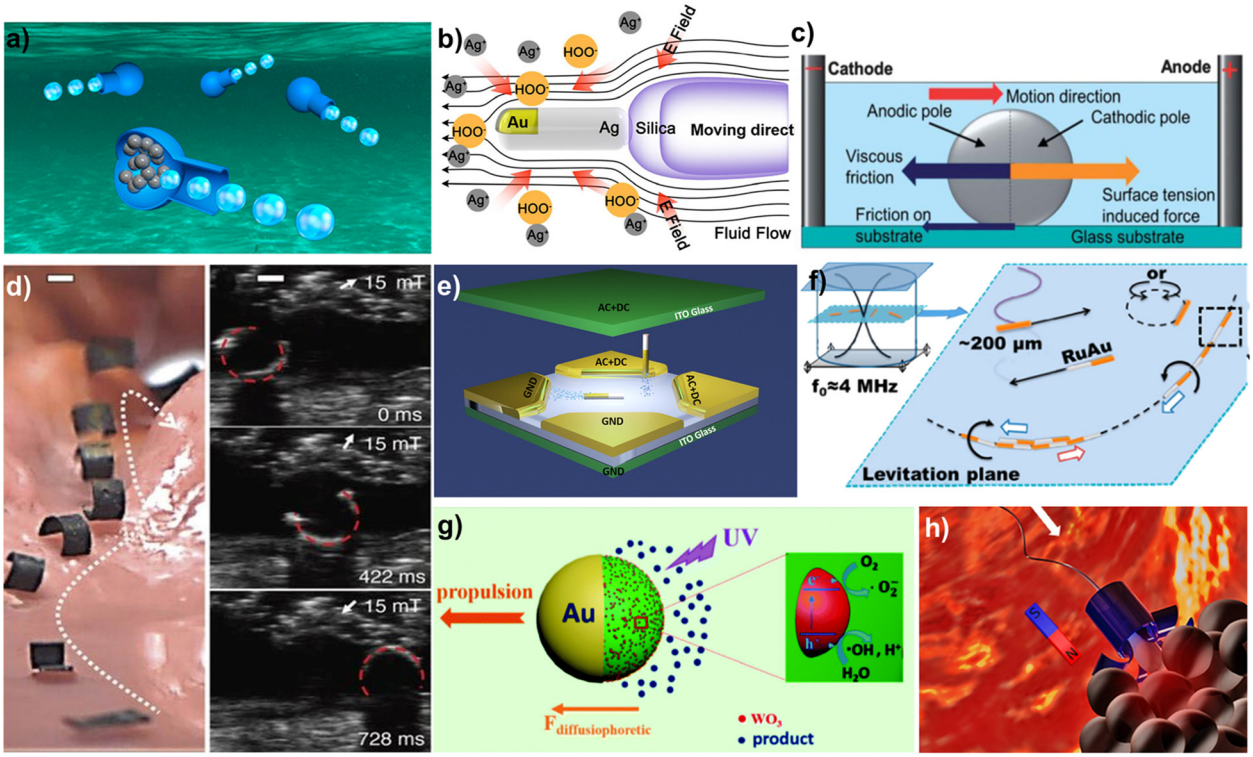

Fig. 1 Different propulsion mechanisms of MNMs. (a) Bubble driven vase MNMs. Reprinted from ref. 43 with permission of the American Chemical Society, copyright 2020. (b) Schematic illustration of MNMs driven by self-diffusiophoresis. Reprinted from ref. 50 with permission of the American Chemical Society, copyright 2022. (c) Schematic illustration of forces for gallium indium alloy liquid metal in alkaline solution. Reprinted from ref. 51 with permission of the Royal Society of Chemistry, copyright 2013. (d) Flexible variable magnetic robot performing crawling motion in the stomach. Reprinted from ref. 56 with permission of Springer Nature, copyright 2018. (e) Electrically driven rod-shaped MNM achieving three-dimensional motion under an electric field. Reprinted from ref. 58 with permission of the American Chemical Society, copyright 2018. (f) Schematic illustration of Au–Ru metal chains performing axial motion along an axial direction in an ultrasonic field. Reprinted from ref. 59 with permission of the American Chemical Society, copyright 2012. (g) Schematic illustration of light driven MNMs. Reprinted from ref. 61 with permission of the American Chemical Society, copyright 2017. (h) Schematic illustration of sperm cell hybrid MNMs. Reprinted from ref. 66 with permission of the American Chemical Society, copyright 2018.

autonomous propulsion of MNMs. For example, Mg/Al-based MNMs have been fabricated based on the reaction of metals with water or acids to produce hydrogen bubbles, and such MNMs are used in the digestive tract *in vivo* in the presence of gastric acid.[44] In addition, due to the enzyme's good catalytic properties and its own biocompatibility, hydrogen peroxidase can also be used to replace platinum for hydrogen peroxide catalyzed bubble actuation.[45,46]

(2) **Phoretic propulsion.** Phoretic propulsion mainly includes self-electrophoresis and self-diffusiophoresis. (1) Self-electrophoresis: the oxidation–reduction reactions are separated in space, electrons are transferred inside the MNMs, and protons are generated and enriched at the anode to form a local electric field.[47,48] For example, on the surface of a gold–platinum bimetallic rod, an electrochemical oxidation half-reaction of hydrogen peroxide occurs at the platinum end, while an electrochemical reduction half-reaction of hydrogen peroxide occurs at the gold end. Due to the asymmetric chemical reactions occurring on the surface of the metal rod, it makes it possible to produce excess hydrogen ions at the end and consume more hydrogen ions at the gold end, which forms a concentration gradient of hydrogen ions from the platinum end to the gold end. Due to the positive charge of hydrogen ions, a higher potential near the platinum end of the metal rod and a lower potential at the gold end was resulted, thus forming an electric field from the platinum end to the gold end. As the metal rods carry a negative charge on their surface in aqueous solution, they will move in the direction of the high potential in the electric field formed by the chemical reaction.[49] (2) Self-diffusiophoresis: when the chemical reaction occurs on the surface of the colloidal particles and a concentration gradient is produced around the particles, the resulting particle movement is called self-diffusiophoresis. In particular, when the reaction occurring on the surface of the particle produces charged ions (electrolytes), the different diffusion coefficients of these ions will result in different distributions of different ions at different locations near the particle and thus may produce an uneven distribution of the electric potential, which in turn produces an electric field driving the motion of the particle and nearby particles[50] (Fig. 1b). The movement of particles produced by such effects is called electrolyte-based self-diffusiophoresis.

(3) **Surface tension gradient propulsion.** When the surface tension of the liquid is high, it will produce a pull on the surrounding liquid with low surface tension, prompting the liquid to move from the area of low surface tension to the area of high surface tension. The distribution of surface tension in the sphere can therefore be altered to create a driven force for the movement of MNMs. For example, as shown in Fig. 1c, by applying an electric field to alter the charge distribution on the surface of a liquid metal, causing an uneven distribution of surface tension to drive the liquid metal. Similarly, a redox reaction between the aluminium sheet-liquid metal (gallium-indium alloy) composite structure and sodium hydroxide can generate a tension gradient that drives the movement of the micro-motor. In addition, there is an important influence of the micromotor's morphology on the surface charge distribution, and thus a surface tension gradient can be achieved to drive the movement of MNM by altering the surface charge distribution. There are also microchannels designed to pass acid and lye respectively on both sides of the liquid metal to achieve uneven charge distribution on both sides, resulting in tension gradient to drive the movement of MNMs.[51]

2.2 External field propulsion

(1) **Magnetic field propulsion.** Magnetic field propulsion is one of the most common driving methods for external field powered MNMs. In nature, there are organisms with self-propulsion capabilities, such as bacteria and sperm cells, that can move through flagella, which have been found to be an efficient form of movement. As a result, researchers have mimicked this flagellar drive to create spiral magnetic MNMs with an externally adjustable rotating magnetic field. Magnetic field-driven MNMs are mainly divided into (1) magnetic particles or rod-shaped MNMs that are subjected to magnetic forces and move under a gradient magnetic field, which can be used for applications such as on-demand navigation to target locations;[52,53] (2) helical MNMs that are driven axially by a rotating magnetic field.[54,55] The rotating magnetic field is generated by a Helmholtz coil and the magnetic MNMs is subjected to movement within the cell in a controlled manner by the rotating magnetic field; And (3) the force generated by the interaction between the MNMs and the substrate is used to drive the movement of the MNMs[56] (Fig. 1d). The peanut-shaped magnetic MNMs can achieve spin-in motion by interacting with the surface substrate under the conical rotating magnetic field generated by the electromagnetic coil set.[57] The advantage of this motion over the previously reported two-dimensional motion is that it can cross obstacles, improving its adaptability to different terrain environments and better application in complex biological environments.

(2) **Electric field actuation.** Electric field actuation is achieved by applying an electric field, and the produced electroosmosis or electrophoresis is used to actuate MNMs. Controlled electric fields are created in three dimensions by adding conductive glass in the *Z*-axis and metal electrodes in the *X*–*Y* plane[58] (Fig. 1e). By changing the distribution of the electric field in different axes, the direction of movement of MNMs can be controlled and the electric field can also be adjusted to carry and release the cargo.

(3) **Ultrasound propulsion.** When an ultrasonic probe is applied to a liquid, there are different pressure nodes in the liquid, resulting in a pressure difference to drive the MNMs towards the pressure nodes. The asymmetric structure increases the pressure difference on the MNMs, which speed up the movement. Wang *et al.* drove the rod-shaped metal robot with ultrasonic waves of MHz frequency. As demonstrated in Fig. 1f, the ultrasound waves emitted at the top interact with the ultrasound waves at the bottom and superimpose, forming a standing wave nodal surface within the liquid surface. The MNMs can move in the standing wave nodule, and the speed can be adjusted by different ultrasonic frequencies. Also, different ultrasonic waves are applied to form a pressure gradient in the liquid, forcing the MNMs to converge in the

area of low pressure. When the ultrasound is switched off, the pressure gradient disappears and the MNMs are rapidly dispersed due to Brownian motion, thus enabling the aggregation and dispersion of MNMs.[59] In addition, ultrasound can be used to trigger the formation of bubbles of easily vaporised material to indirectly drive the movement of the MNMs, and the movement can be controlled by turning the ultrasound on and off.[60]

(4) Light propulsion. Light can be found everywhere in nature, so light-driven MNMs are used in a wide range of applications. The mechanism of light-driven MNMs is divided into three main categories: photocatalytic self-diffusiophoresis, photocatalytic self-electrophoresis and self-thermophoresis. (1) Photocatalytic self-diffusiophoresis:[61] when light is shone on the surface of the MNMs, the surface material will undergo a photocatalytic reaction or photodecomposition reaction to release product ions (Fig. 1g). (2) photocatalytic self-electrophoresis:[62] when light irradiates a MNM with photocatalytic capability (*e.g.* TiO_2–Au), hole–electron pairs will be generated and the holes will be distributed on the semiconductor side (TiO_2) for oxidation with water, while the electrons will migrate to the metal side (Au) and reduce H^+ to H_2. (3) Self-thermophoresis:[63] when the surface of the MNM is covered with a photo-thermal material (*e.g.* Au), a local temperature gradient field will be formed around the MNM due to the photo-thermal effect, thus forming local convection to drive the MNM in the opposite direction. So far, light driven MNMs that can react to various wavelengths of light exposure have been developed. Generally, these light propelled MNMs consisting of TiO_2 can only be stimulated by ultraviolet (UV) light, which has adverse health effects. Therefore, the development of visible light or near-infrared (NIR) driven MNMs is essential for their biomedical and environmental applications. For example, Cai *et al.*[64] demonstrated the fabrication of Janus micromotors responsive to blue and green light by utilizing bismuth oxyiodide (BiOI), a material known for its exceptional photocatalytic activity. Given the ability of NIR laser irradiation to penetrate biological tissues with minimal absorption, MNMs that can be stimulated by NIR irradiation have potential application in biomedicine. Most NIR-driven MNMS can be driven relying on thermophoretic mechanisms. Recently, a new type of nanomotor, namely AuNR–SiO_2–Cu_7S_4, has been developed to combat bacterial infections through active treatment.[65] These nanomotors are driven by NIR-II light, utilizing the thermal gradient generated at the AuNR–Cu_7S_4 interface.

2.3 Biological agent propulsion

Biohybrid MNMs can be produced by combining motile biological agents, such as sperm cells, bacteria, and some microorganisms. Since motile biological agents are very biocompatible, they have good prospects in the field of drug delivery and medical testing. However, the poor control of natural motile cells does not allow for good target delivery and other intended goals. Therefore, there is a need to improve their control performance by combining them with external auxiliary structures in order to better fulfil their intended tasks. The researchers combined sperm cells with magnetic nanocapsules to create biohybrid MNMs that can be controlled in the direction of their motion through an external magnetic field[66] (Fig. 1h). The flagellar motion of the sperm cells drives the overall movement of the motor. Magnetic micrometer cone tubes can be produced through self-curling and contain sperm cells to form biohybrid MNMs. Additionally, magnetic flower-like structures can be fabricated through photolithographic processing. The large specific surface area of the sperm cell head enables the loading of drugs and allows for controlled release of the drug at the target site. Recently, ALG@yeast-Fe_3O_4 BioBots, capable of magneto- and catalytic functionalities, have been constructed by encapsulating Fe_3O_4 nanoparticles and yeast cells within an alginate polymer matrix.[67] The continuous oscillatory motion of the BioBots in the solution is induced by CO_2 gas from the catalytic fermentation of sugars. With the ability for movement, the BioBots promote the production of alcohol. An intriguing instance involves the fabrication of self-drilling seed carriers, wherein wood veneer is transformed into rigid and biodegradable hygromorphic actuators exhibiting an exceptionally large bending curvature.[68] The autonomous self-burying carrier has the capability to accommodate seeds of various sizes as well as biofertilizers, offering potential benefits in enhancing the efficiency of aerial seeding and alleviating agricultural and environmental pressures.

3. Sensing application of MNMs and related principles

3.1 Intelligent sensing based on the motion behavior analysis of MNMs

Self-driven motion is a crucial characteristic of MNMs. Since their invention, researchers have extensively studied their motion behavior and mechanisms. Through these efforts, it has been discovered that various substances can have an inhibiting effect on the motion of certain MNMs, and this has been leveraged to develop sensing methods based on changes in the motion of these motors. This section will present the applications of MNMs for sensing metal ions, organic or polymeric substances, and microorganisms, as determined by their unique response mechanisms.

3.1.1 Ion response. As shown in Fig. 2a, the bimetallic gold-platinum nanomotor moves axially due to the varying catalytic responses of platinum and gold to the redox of hydrogen peroxide. The researchers discovered that in the presence of silver ions, the nanomotor's speed significantly accelerates, while the presence of other ions such as lead, manganese, nickel, and copper slowed down the nanomotor.[69] This is because silver ions deposit onto the nanomotor's surface in the presence of hydrogen peroxide, thereby enhancing its catalytic activity. In contrast, some heavy metal ions inhibit the catalytic activity of the metal atoms on the nanomotor's surface. Based on the acceleration or deceleration of the nanomotor's response to different ions, the corresponding ion sensors can be prepared, and the quantitative detection of these ions can be achieved by analyzing the nanomotor's

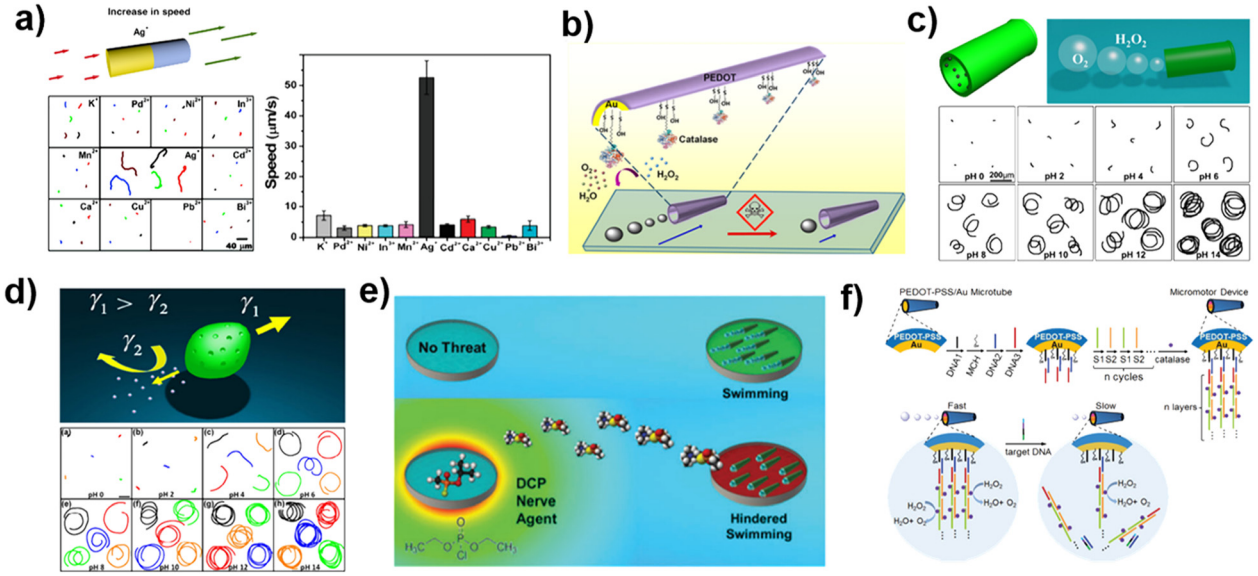

Fig. 2 Sensing based on the motion behavior analysis of MNMs. (a) Metal ion response using gold-platinum nanomotors based on motion changes. Reprinted from ref. 69 with permission of the American Chemical Society, copyright 2009. (b) Scheme illustrating the pollutant inhibiting the activity of catalase powered micromotors. Reprinted from ref. 25 with permission of the American Chemical Society, copyright 2013. (c) pH responsive bullet-shell motor based on motion changes. Reprinted from ref. 71 with permission of the American Chemical Society, copyright 2016. (d) Spindle-shaped motor for pH sensing based on motion change. Reprinted from ref. 72 with permission of Springer, copyright 2016. (e) The detection of diethylphosphoacyl chloride was achieved by peroxidase powered motors. Reprinted from ref. 74 with permission of the Royal Society of Chemistry, copyright 2016. (f) Micromotors for DNA detection based on motion changes. Reprinted from ref. 77 with permission of the Royal Society of Chemistry, copyright 2017.

trajectory and its motion speed. In another example, Janus micromotors made of PCL/Mg have been developed to detect precious metal ions by monitoring changes in their motion. These micromotors, created through a displacement reaction between Mg and the precious metal ions, exhibit movement in a hydrogen peroxide solution. The speed of motion is notably affected by the types and concentrations of the metal ions, allowing the micromotors to function as motion-based sensors for metal ions.[70]

In recent years, enzyme-driven MNMs have become a significant area of research in MNM technology, due to their excellent propulsion capability and biocompatibility. These MNMs can utilize hydrogen peroxidase and urease, powered by hydrogen peroxide and urea respectively, to drive their own motion. However, common heavy metal ion contaminants, such as Hg^{2+} and Cu^{2+}, often have a negative impact on enzyme activity. In the case of hydrogen peroxidase, the enzyme's sulfhydryl and amino groups can bind to mercury and copper ions, respectively, forming complexes that alter the structure of the biological enzyme. This will result in a significant reduction of enzyme activity and a decrease in the movement speed of the MNMs (Fig. 2b). Therefore, the presence of heavy metal ions in a solution can be quantified based on the speed change of the enzyme-driven MNMs.[25]

In addition to metal ions, changes in the motion behavior of MNMs can also be used for hydrogen ion detection, or pH sensing. This is demonstrated in Fig. 2c, which shows a bullet-shell shaped MNM with a gelatin shell and an internal load of platinum nanoparticles. The MNM undergoes self-driven in a hydrogen peroxide solution based on a bubble-propelled mechanism. The researchers found that the motion of these nanomotors was impacted by pH, with motion speed increasing as the pH increased in the range of 0–14. This was due to the combination of the different structure of the gelatin and the catalytic effect of the platinum nanoparticles at various pH levels. As the pH increases, the opening of the gelatin shell widens, the frequency of bubble production increases, and the propulsive effect strengthens. At low pH, the platinum nanoparticles catalyze the direct cleavage of the hydrogen peroxide molecule into two hydroxyl radicals, creating a concentration difference at the ends of the bullet-shell motor, which is driven by self-diffusiophoresis. At high pH, the platinum nanoparticles catalyze the production of oxygen from hydrogen peroxide, which is driven by more effective bubble recoil. With the dual pH response of the gelatin structure and the catalytic properties of the platinum nanoparticles, the MNM can achieve pH-sensitive sensing detection.[71]

In addition to the sensing approaches that alter the motion behavior of MNMs through changes in their chemical reactivity, there are also novel structural and material designs for MNMs that can be used for sensing and detection. As illustrated in Fig. 2d, researchers have utilized electrostatic spinning to create a spindle-shaped motor made of polycaprolactone and sodium dodecyl sulfate (an anionic surfactant). This motor releases the surfactant slowly into solution, resulting in a change in the local surface tension. The Marangoni effect causes the motors to move towards the side with higher surface tension. This movement is greatly influenced by the surface tension of the liquid, and thus, the liquid environment can have a significant impact. In this study, the surface tension of

water was found to have nothing to do with pH; however, the surface tension of the surfactant solution was affected by pH. As the pH increases, the surface tension between the surfactant solution and the MNM decreases, leading to an increase in the driving force of the motor and an increase in its motion speed, thus completing the pH sensing based on motion speed analysis.[72]

3.1.2 Organic substance/macromolecule response. MNMs are attracting significant research interest for their potential applications in biomedical detection due to their miniature size and ability to move autonomously. As a result, researchers have been working to develop methods and devices that can sense and detect certain organic substances or macromolecules by monitoring the motion behavior of these MNMs.

Some organic molecules have been found to have a negative impact on the performance of MNMs that use hydrogen peroxide as fuel. This is because the organic molecule reacts with the hydroxyl radicals, intermediates in the catalytic breakdown of hydrogen peroxide, and scavenges them in both the bubble driven and self-diffusiophoresis driven mechanisms, preventing the MNMs from generating sufficient driving capacity. As the organic molecule concentration increases, the movement speed of the MNM decreases. And beyond a certain point, it loses its motion properties. The presence of a high concentration of blood proteins also significantly affects the movement of MNMs, particularly in the case of platinum-based nanomotors. The proteins bind to the platinum nanoparticles through their sulfhydryl groups and adsorb directly onto the surface of the motor, which prevents contact between the surface catalyst and fuel source, reducing the motor's active sites and inhibiting its motion. By analyzing the motion response of the MNMs to these organic or biological macromolecules, smart sensor devices can be developed.[73] However, it is important to consider the interaction between various substances and the accuracy. The specificity of the detection can be improved through specific pre-treatment or the design of the MNM's structure and materials.

The conformation of biological enzymes, which determines their catalytic activity, can be altered by various factors such as temperature, pH, and the presence of inorganic or organic molecules. As a result, MNMs powered by enzyme can respond to environmental changes and specific substances, as reflected by changes in their motor behavior. As an example, Fig. 2e shows a study in which researchers created a MNM made of a composite of peroxidase and polyethylene dioxythiophene/gold particles.[74] The motor was able to detect the presence of diethylphosphoryl chloride (DCP), a neurotoxin, in a gaseous environment. DCP is harmful to peroxidase and reduces the movement speed of the MNM. These neurotoxin detection devices based on MNMs have low detection limits and high selectivity and sensitivity, making them suitable for both military and civilian applications. In another example, the same peroxidase-driven micromotor can be used to detect pesticide residues in vegetables, promising for monitoring food safety in everyday life.[75]

The motion behavior of MNMs can also be used for DNA detection. For example, the micromotors powered by Pt nanoparticles functionalized through DNA were reported to motion-based sense for DNA.[76] The works in which using enzymes instead of Pt nanoparticles to power micromotors have also been reported. As illustrated in Fig. 2f, researchers have developed a hydrogen peroxide-driven polyethylene dioxythiophene/gold particle composite tubular micromotor that includes a specially designed group of nucleic acid chains. These chains compete with one another, and when the target nucleic acid chains are present, they cause the hydrogen peroxides-modified nucleic acid chains to be removed. The amount of target nucleic acid can then be determined by analyzing the reduction in the MNM's speed of movement.[77] The same group fabricated catalase powered microtubes by DNA conjugate for DNA sensing. The presence of the target DNA induces the release of catalase modified DNA, which reduces the micromotor speed.[78] So, the speed of the micromotors can be used to quantify DNA in solution. To improve the detection sensitivity, DNA self-assembly and umbrella-shaped structure were used to construct the enzyme-driven micromotors.[79] In another example, the motion of micromotors was detected by immobilizing a pH-sensing FRET-labeled triplex DNA nano-switch onto urease-powered micromotors.[80] While undergoing self-propulsion, the decomposition of urea induced a rapid increase of pH. The resulting pH alteration was continuously monitored in real time by evaluating the FRET efficiency through confocal laser scanning microscopy at different time intervals. In order to facilitate data collection and analysis, making the monitoring process more convenient and efficient, the smartphone is used to analyze the motion of micromotors. Shafiee *et al.* combined cellphone-based optical sensing with micromotor motion to achieve molecular detection of HIV-1.[81] The presence of HIV-1RNA results in the formation of large-size amplicons, which reduce micromotor speed. The micromotor speed was detected and analyzed by the mobile phone system to analyze the HIV-1 RNA concentration in real time. The glutathione caused the catalytic layer being poisoned by the formation of a thiol bond and the decrease of speed in graphene-wrapped/PtNPs Janus micromotors.[82] Integrating with smartphones, the glutathione can be detected by naked-eye visualization. miRNA is a class of small non-coding RNA molecules that can regulate gene expression at the post-transcriptional level. Abnormal expression of miRNA is closely associated with the occurrence and development of various diseases, including cancer, cardiovascular diseases, and neurological disorders. The detection of miRNA is of great significance for understanding gene regulation and disease research. Oksuz *et al.*[83] immobilized single-stranded DNA on W_5O_{14}/PEDOT-Pt micromotors to detect miRNA by fluorescence signal and motion change.

The motion behavior of MNMs can be utilized in a variety of sensing applications, ranging from specific ions and molecules to biomolecules. The modulation of the MNM's movement is typically caused by changes in its catalytic activity, a reduction in the number of catalytic sites, or specific structural design. Researchers have developed various MNM designs for different sensing applications, such as environmental detection,

biomedical sensing, and food safety. However, challenges remain in terms of achieving consistent and accurate results, making it necessary for further research and development in the field.

3.2 Intelligent sensing of MNMs based on optical detection methods

Optical detection is a sensing technique that utilizes spectroscopic information, such as spectral band, light intensity, or lifetime, for qualitative or quantitative analysis of the target. With the advancements in optical instrumentation, the precision, accuracy, and sensitivity of optical detection methods have improved significantly and are now crucial for detecting inorganic small molecules, biological macromolecules, and microorganisms. In this section, we will discuss the application of MNMs in colorimetric and fluorescence methods, as well as their use in combination with electrochemiluminescence detection and Raman-enhanced spectroscopy.

3.2.1 Colorimetric methods. Colorimetry is a technique for determining the type and concentration of a substance by comparing the color of a solution or measuring its absorbance. This method is typically performed by analyzing UV-Vis, fluorescence, and infrared spectra. The use of MNMs in colorimetry increases sensitivity and reduces detection time compared to traditional methods, as the MNMs are in close and frequent contact with the target. Fluorescence quenching is a commonly used principle in colorimetric MNM sensing applications. There are also applications that utilize shifts in the spectrum on the MNM for detection. MNM are loaded with special probe molecules that undergo structural changes when exposed to the target, leading to shifts in UV-Vis or IR spectra. The MNM accelerates the interaction between the molecule and the target, increasing reaction efficiency and detection accuracy.

Ma *et al.* aimed to automate the process of enzyme-linked immunosorbent assay (ELISA) by developing a maneuverable immunoassay probe based on magnetic nanorobots (Fig. 3a). The probes, known as magnetically maneuverable immunoassay probes (MNR-Ab1s), were constructed by decorating capture antibodies on the surface of rod-like, magnetically driven nanorobots. To facilitate the assay, a detection unit consisting of various functional wells was fabricated using 3D printing technology. When exposed to a magnetic field, the probes can actively rotate and move between the functional wells, resulting in improved binding efficacy and shorter assay time from a few hours to less than half an hour, compared to traditional ELISA detection methods.[84] The combination between micromotors and immunoassay has also been reported in another work. The bubble-propelled micromotors have been designed for competitive immunoassays, enabling fast and visible identification of the target analyte (cortisol).[85]

The works about colorimetric detection of targets using peroxidase activity of motor materials have also been reported. For example, Escarpa *et al.*[86] fabricated tubular micromotors composed of a hybrid single-wall carbon nanotube (SW)–Fe_2O_3 outer layer, along with a MnO_2 catalyst. Through catalytic

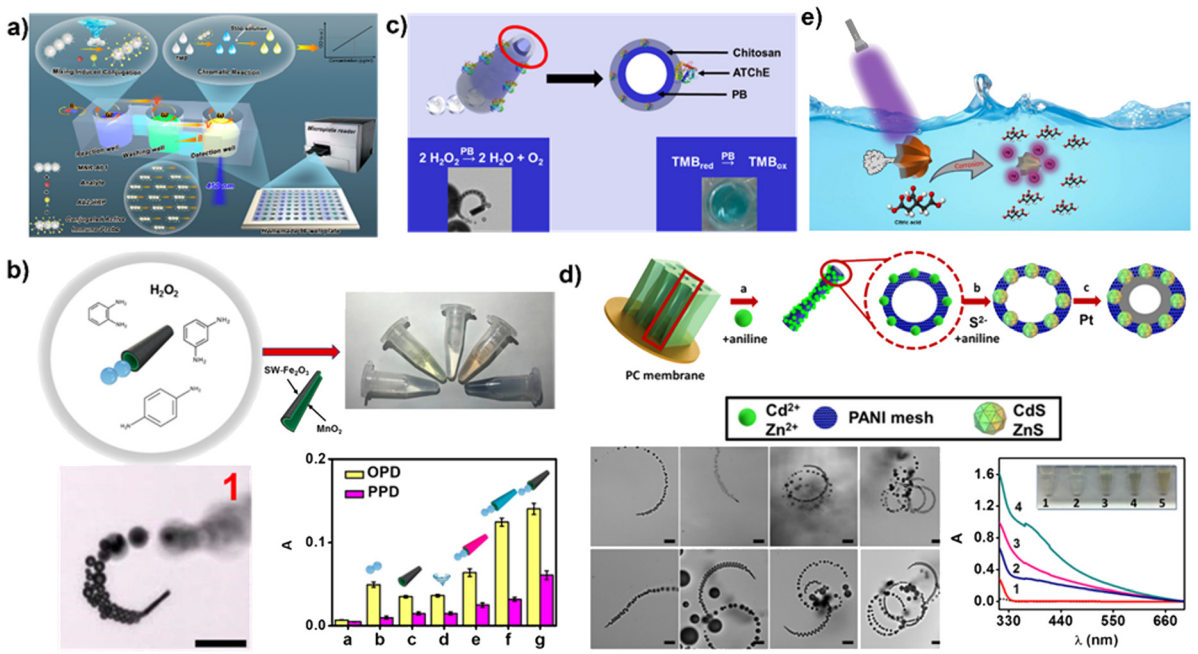

Fig. 3 Enhanced colorimetric sensing using MNMs. (a) Automated and efficient ELISA analysis based on magnetic nanorobots. Reprinted from ref. 84 with permission of the American Chemical Society, copyright 2022. (b) Naked-eye sensing of phenylenediamine isomers using bubble powered micromotors. Reprinted from ref. 86 with permission of the American Chemical Society, copyright 2018. (c) Neostigmine determination by tubular micromotors with enzyme mimetic activity. Reprinted from ref. 87 with permission of the American Chemical Society, copyright 2022. (d) ZnS-PANI-Pt micromotors for colorimetric detection of Hg^{2+}. Reprinted from ref. 88 with permission of the American Chemical Society, copyright 2016. (e) Light powered Pt/Ag_3VO_4 micromotors for sensing citric acid. Reproduced from ref. 89 with permission of Elsevier, Copyright 2022.

decomposition, hydrogen peroxide yields oxygen and hydroxyl radicals. The oxygen facilitates the movement of the micromotors, while the hydroxyl radicals react with phenylenediamine isomers to generate a colorful solution, enabling the rapid and colorful detection of phenylenediamine isomers (Fig. 3b). In another work, the same group utilized Prussian blue/chitosan micromotors and functionalized them with acetylthiocholinesterase enzyme (ATChE) to enable colorimetric determination of the nerve agent neostigmine[87] (Fig. 3c).

The micromotors incorporate specific materials that react with the targets, resulting in color generation for detection purposes. Furthermore, the micromotors' movement enhances their interaction with the targets, thereby increasing the sensitivity of detection. Escarpa *et al.*[88] cross-linked ZnS and CdS nanoparticles onto polyaniline (PANI)–Pt micromotors. During micromotor movement, Hg^{2+} will replace Zn^{2+} to produce HgS–PANI–Pt micromotors, which appear bright yellow, so the ZnS–PANI–Pt micromotors can be used for dynamic visible discrimination of Hg^{2+} (Fig. 3d). In addition, Pt/Ag_3VO_4 micromotors powered by light have the capability to release Ag nanoparticles when exposed to citric acid[89] (Fig. 3e). As a result, the surface plasmon resonance of the Ag nanoparticles depends on the concentration of citric acid.

3.2.2 Fluorescence method. Fluorescence quenching, which is still in the realm of colorimetric methods, has gained significant attention for its potential applications in MNM sensing. Fluorescence quenching is a phenomenon that occurs when a luminescent material such as a fluorescent molecule or quantum dot undergoes a reduction in the fluorescence intensity or fluorescence lifetime under certain conditions. This phenomenon has been widely utilized for sensing purposes, with one example being the detection of mercury ions in water environments using carbon quantum dots. MNMs can also be modified with specific fluorescent molecules or quantum dots, enabling them to detect specific ions or molecules. For example, the fluorescent CdTe quantum dots[90] and acridine orange,[91] which can be quenched by Hg^{2+}, are incorporated into the MNMs to enhance the ability for detecting Hg^{2+}. Fig. 4a demonstrates the modification of one side of a silica/platinum motor with fluorescein, a green fluorescent organic molecule. This molecule is highly responsive to neurotoxins, such as sarin and pokeweed, and rapidly loses its fluorescence properties within ten seconds.[92] This ''light-up-light-down'' fluorescence design allows for a qualitative measurement of the presence of the specific molecules. Numerous studies have reported the utilization of fluorescent quantum dots, covalent-organic-framework, upconverting nanoparticle, fluorescein isothiocyanate (FITC), and Eu-MOF functionalized micromotors for detecting a wide range of substances, including endotoxins,[93] explosives,[94,95] gases,[96] and metal ions[97,98] such as Cu^{2+} and Fe^{3+}. The MNM's motion enables a swift and efficient response of the fluorescent substance to the target, dramatically lowering the detect concentrations (as low as 0.07 ng mL^{-1} of endotoxin) and shorting the detection time to 15 min compared with several hours required by the existing Gold Standard method.[83] Similarly, the COF-functionalized micromotors can

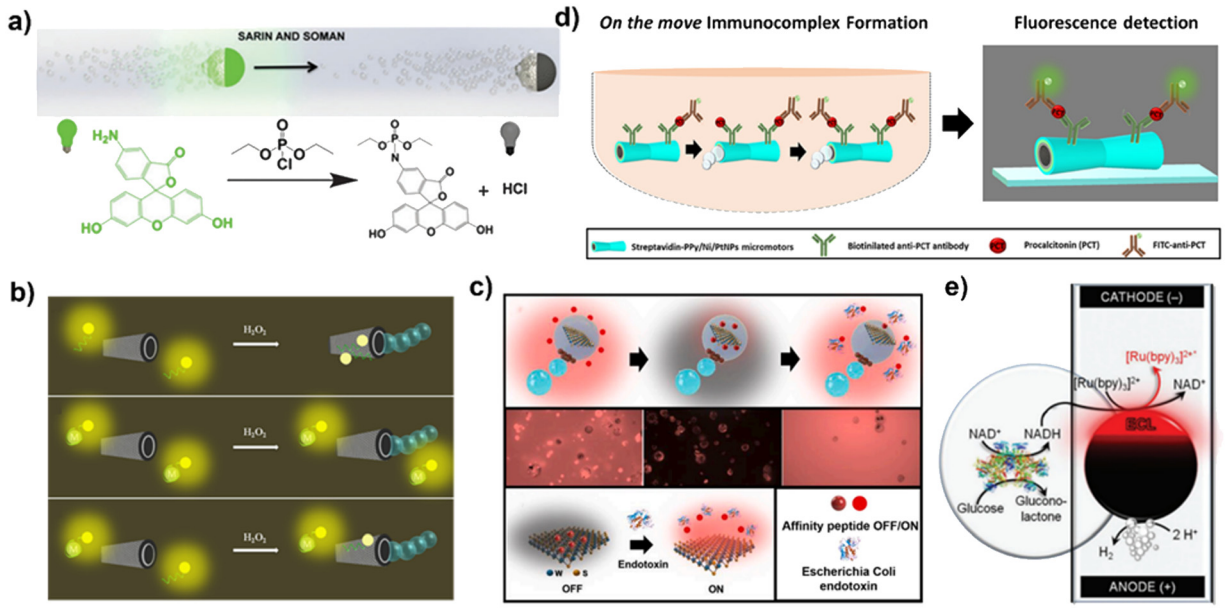

Fig. 4 Enhanced fluorescence and electrochemiluminescence sensing using MNMs. (a) A MNM sensing application using the fluorescence quenching mechanism. Reprinted from ref. 92 with permission of the Royal Society of Chemistry, copyright 2015. (b) A MNM sensing application using the fluorescence ''OFF–ON'' mechanism. Reprinted from ref. 99 with permission of the American Chemical Society, copyright 2017. (c) The detection of bacterial lipopolysaccharides using WS_2–Pt–Fe_2O_3 polycaprolactone Janus micromotors. Reproduced from ref. 103 with permission of Elsevier, Copyright 2020. (d) The detection of procalcitonin combining micromotors and fluorescence immunoassay. Reprinted from ref. 106 with permission of the American Chemical Society, copyright 2020. (e) The electrochemiluminescence-based glucose detection by MNMs. Reprinted from ref. 108 with permission of the Royal Society of Chemistry, copyright 2014.

detect the 5 ppm 2,4,6-trinitrophenol within 10 min. This makes it highly practical for use in critical areas such as food safety and environmental monitoring.

A MNM sensing application using the fluorescence "OFF–ON" mechanism is presented in this example. As depicted in Fig. 4b, researchers have developed a tubular MNM that has an outer layer of graphene oxide and an inner layer of platinum nanoparticles. An aptamer with a fluorescent group is initially adsorbed onto the outer graphene oxide layer. The fluorescence is quenched by the graphene oxide, but the aptamer can specifically bind to the fungal toxin (target molecule). This binding causes the fluorescent group to be "dragged" away from the surface of the graphene oxide, so the fluorescence restores. The quantity of mycotoxin can then be determined by measuring the fluorescence intensity.[99] Based on the same detection strategy, graphene oxide coated micromotors which can be driven by bubble are developed to detect toxin,[100] ricin[101] and interleukin-6 (IL-6).[102] In another examples, WS_2 that is coated on the surface of micromotors acts as quencher of fluorescent dyes.[103,104] Escarpa *et al.*[103] incorporated a rhodamine-labeled affinity peptide within WS_2–Pt–Fe_2O_3 polycaprolactone Janus micromotors (Fig. 4c). The introduction of WS_2 induces quenching of the rhodamine-labeled affinity peptide, while the binding of bacterial lipopolysaccharides to the affinity peptide prompts its detachment from the micromotors' surface, effectively restoring fluorescence. The extent of fluorescence enhancement directly correlates with the concentration of bacterial lipopolysaccharides. In addition, a smartphone device combined with micromotors was developed to enable real-time fluorescence assays.[105]

Fluorescence immunoassay is a method used to detect and quantify specific analytes, such as proteins or antibodies, by employing fluorescent labels. Fluorescence immunoassay offers advantages such as high sensitivity, quantitative analysis, multiplex detection, and real-time monitoring. However, it has limitations in terms of instrument cost, sample handling, automation requirements, and background interference. To overcome these limitations, Escarpa *et al.*[106] have developed tubular micromotors powered by bubbles, integrated with fluorescence immunoassay, for the detection of procalcitonin, which is a biomarker used in early sepsis diagnosis (Fig. 4d). In another example, Zhao *et al.*[107] showcased the application of structural color barcode micromotors in multiplex assays by change of fluorescence. These micromotors were created by injecting a hydrogel containing platinum (Pt) and ferric oxide (Fe_3O_4) into a stomatocyte colloidal crystal, which exhibit structural color. When hydrogen peroxide is present, the motion of these structural color motors speeds up the binding between the probe and the target, thus enhancing the overall detection process.

3.2.3 Electrochemiluminescence method. Electrochemiluminescence is a process that involves the generation of new substances through electrochemical reactions in an electrolyte solution. These substances can then emit light through interactions with other substances in the solution. This analytical method, which blends electrochemical and chemical techniques, has the advantages of high selectivity and sensitivity, and has developed rapidly in recent years in the fields of immunoassay and nucleic acid detection. With ongoing research into the functionalization of MNMs, electrochemiluminescence has been integrated into their sensing applications, further enhancing their capabilities.

As shown in Fig. 4e, researchers have designed a glucose detection device consisting of glassy carbon microbeads and vertical capillaries with electrodes attached at both ends. The capillaries contain inorganic complexes for electrochemiluminescence containing ruthenium and the auxiliary reactant tri-*n*-propylamine. During the detection process, the glassy carbon microbeads undergo an asymmetric chemical reaction in the presence of an electric field. At the cathode end of the microbeads, the reduction of hydrogen ions occurs, and at the anode end, the oxidation of glucose and the conversion of the co-enzyme NAD^+ to reduced co-enzyme NADH takes place, participating in the electrochemiluminescence of the ruthenium-containing complex, thereby completing the luminescence and coenzyme cycle. The luminescence intensity produced during the electrochemiluminescence is highly correlated with the initial glucose concentration, allowing for the effective monitoring of glucose levels.[108]

The electrochemiluminescence-based sensing method has the advantages of high sensitivity, wide linear range, and simple equipment, making it a promising candidate for use in the development of next-generation portable biosensing devices. However, the complex principle of electrochemiluminescence testing requires further research and development before it can be effectively integrated into the field of MNM-based intelligent sensing.

3.2.4 Raman-enhanced spectroscopy method. The surface Raman enhancement effect is a phenomenon that amplifies the Raman scattering signal on rough metal surfaces such as gold, silver, and copper, or in the gaps between metal nanoparticles. This technique, known as surface Raman-enhanced spectroscopy (SERS), possesses the benefits of conventional Raman spectroscopy, including simplicity, non-destructiveness, and the ability to detect specific molecular structures. As a result, it can sense even low concentration of target molecules with exceptional sensitivity. The emergence of SERS has greatly broadened its applications in areas such as medical testing, environmental monitoring, and material analysis. Additionally, the Raman-enhanced "hot spot" probes on the surface of MNMs, which can move under external fields, allow dynamic enrichment of Raman signals and detection of micro-regions at target sites.

The researchers have developed active SERS probes based on micro/nano-robots with autonomous motion and precise control. The SERS-enhanced probes were constructed using silver nanowires as the main structure, coated with a silica shell layer and formed AgCl-powered driving mechanism. The design of the micro/nano-robotic propulsion and detection was ingeniously integrated to achieve controlled aggregation in target locations using phototaxis of the micro/nano-robot.[109] This was a pioneering achievement in the systematic validation of the

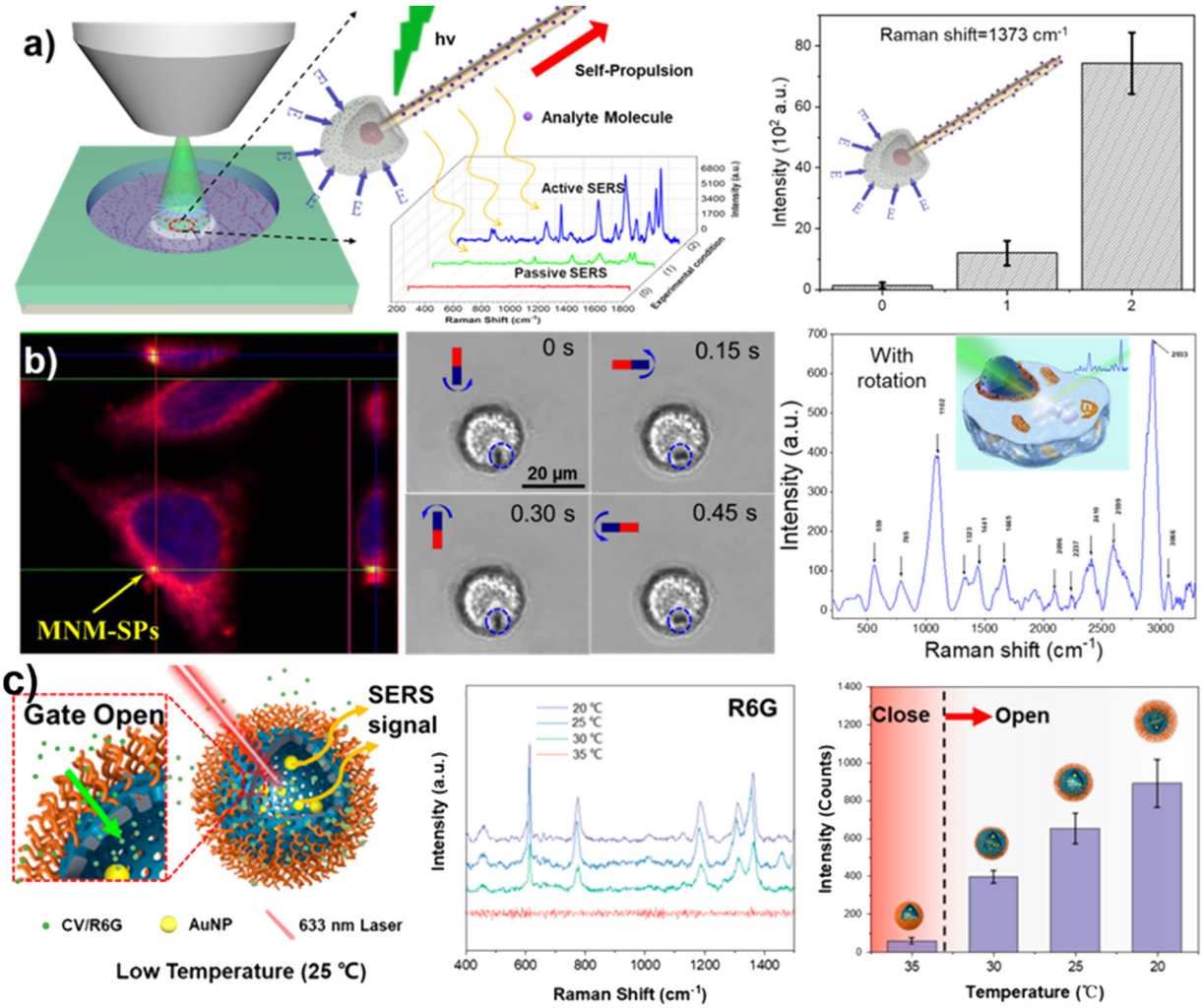

Fig. 5 Small molecule sensing using MNMs based on SERS. (a) *In vitro* Raman sensing of a one-dimensional photocatalytic micro–nano robot. Reproduced from ref. 109 with permission of Wiley, Copyright 2018. (b) Magnetic rod-shaped nanorobot for intracellular signal detection. Reproduced from ref. 110 with permission of American Association for the Advancement of Science, Copyright 2020. (c) A temperature responsive nanomotor for active micro-sampling. Reprinted from ref. 112 with permission of the American Chemical Society, copyright 2022.

MNM based SERS probe's feasibility for early tumor detection (Fig. 5a). To optimize the control accuracy of the MNMs, a magnetic rod-like MNMs with silver nanoparticles grown *in situ* on the rod-like structure was designed and developed. This magnetic nanorobot, serving as an active and smart SERS probe, provided high sensitivity through active and precise targeting at the micro/nano-scale for self-cleaning and targeted intracellular signal detection (Fig. 5b).[110] In another example, plasmonic nanostructure hotspots have been integrated into tubular micromotors through nanoimprint and rolling origami techniques. The magnetic motion of these micromotors enhances molecular enrichment, resulting in an amplified surface-enhanced Raman scattering (SERS) signal.[111] Furthermore, a temperature-responsive microsampling nanorobot also was developed by encapsulating metal (Au) nanodots inside hollow mesoporous silica nanoparticles and then grafting a temperature-responsive polymer, on their external surface[112] (Fig. 5c).

In this section, we highlighted some of the sensing applications of MNMs that utilize optical detection methods. Optical detection methods are widely popular in portable detection devices due to their ease of use and precision. By integrating the motion properties of MNMs with optical sensing methods, the detection capabilities of optical detection methods have been greatly enhanced. Additionally, the innovative structural designs of MNMs have expanded the scope of application for optical detection methods.

3.3 Intelligent sensing of MNMs based on electrochemical analysis methods

Electrochemistry is a sensing technique that utilizes the measurement of electronic charge transfer during redox reactions on an electrode surface. When operating in an electrolyte solution, alterations in the electrode surface can be effectively detected through signals such as microcurrents, impedance, and photoelectric conversion. The method is highly adaptable

to various environments and does not require complex testing equipment, making it a valuable option for the development of miniaturized and portable sensing devices. With recent advancements in MNMs, new sensing methods have emerged that utilize their propulsion behavior to improve the performance of electrochemical detection in the field of electrochemical sensing.

MNM sensing using electrochemical analysis is a cutting-edge technique that has emerged in recent years and operates on similar principles, typically utilizing cyclic voltammetry (CV) or electrochemical impedance spectroscopy (EIS) for qualitative analysis of electrode surface reactions. Precise quantitative analysis of the substance can be performed through differential pulse voltammetry (DPV, Fig. 6a).[113] MNMs play a crucial role in this technique *via* enriching and delivering the substance. This section highlights the advancements in the use of MNMs in electrochemical testing.

Bubble-propelled MNMs have been demonstrated to enhance the mixing of fluids and the transport of substances, improving the efficiency in conventional chemical reactions, and making a significant contribution to electrochemical sensing. The magnesium-based Janus MNM, for instance, generates substantial micro-bubbles in water, which greatly facilitate mass transfer and local convection in the solution.[114] The working electrode is modified with a substrate that can interact with the substance to be detected, for example, glucose oxidase on a glassy carbon electrode used to detect glucose in solution. The oxidation peak of the substrate can then be quantified through CV and DPV curves (Fig. 6b). The signal strength and sensitivity of electrochemical blood glucose detection are enhanced by accelerating the redox rate of reactant molecules on the electrode and improving mass transfer in the solution.

Some MNMs have been shown to increase the sensitivity of sensing through their catalytic effect on the substrate, converting it from a low electrochemically active substance to a high electrochemically active substance. Escarpa *et al.*[115] also utilized Mg/Au Janus micromotors for the degradation and electrochemical analysis of diphenyl phthalate (DPP). In the chloride-enriched samples, the Mg/Au Janus micromotors move and produce hydrogen as well as hydroxyl radicals, which degrade DPP to phenol. The determination of phenols can be accomplished through differential pulse voltammetry, while the movement of micromotors enhances fluid mixing, thereby increasing the sensitivity of detection.

In recent years, researchers have not only improved the performance of MNMs but also functionalized them by modifying their surfaces. This enables the MNMs to perform more complex tasks. As depicted in Fig. 6c, when an antibody is modified on the surface of a MNM, the functionalized MNM can actively capture the antigen through its motor behavior when added to the substrate solution. This active capture is more efficient than passive capture that relies on molecular diffusion. A large number of magnetic nanoparticle-based MNMs have been used in electrochemical sensing. Magnetic field-driven silica-coated ferric tetroxide nanomotors with IgG antibodies have been prepared. These MNMs driven by magnetic field can trap the free antigen in solution, which can then be collected on the surface of a working electrode under the

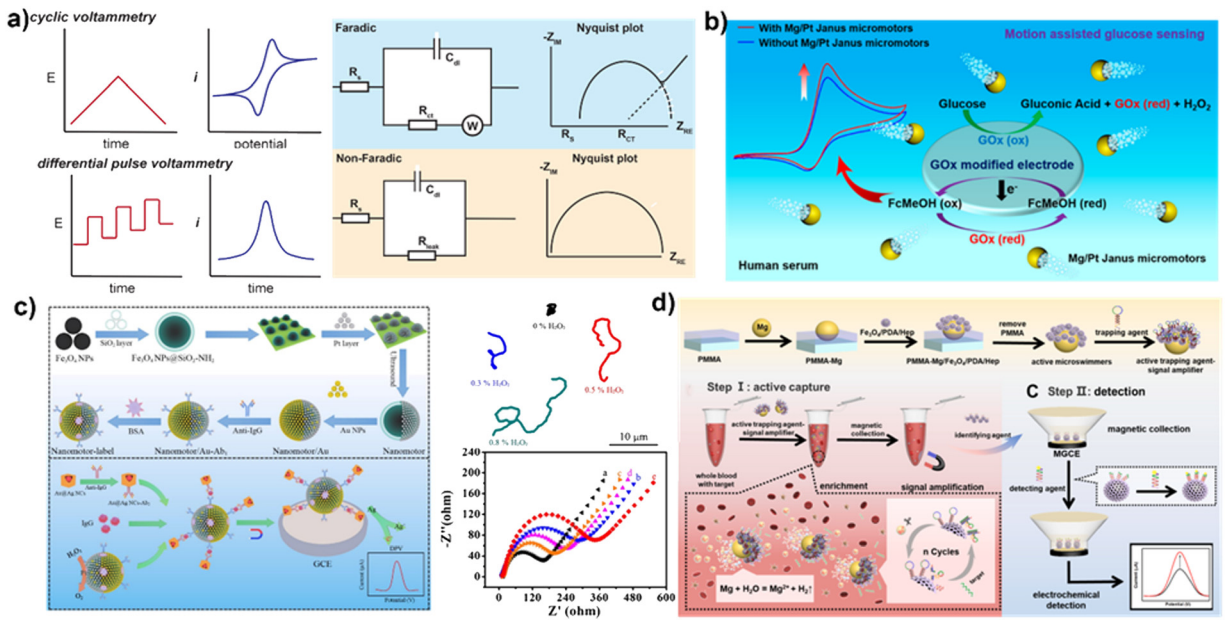

Fig. 6 Sensing application using MNMs based on electrochemical analysis. (a) The amplification of signals in electrochemical sensing processes. Reprinted from ref. 113 with permission of the American Chemical Society, copyright 2019. (b) MNMs for catalytic reactions with substrates to electrochemical activity and electrochemical signal enhancement. Reprinted from ref. 114 with permission of the American Chemical Society, copyright 2019. (c) The fabrication of a self-assembled sandwich immunosensor. Reprinted from ref. 116 with permission of Springer, copyright 2022. (d) The active trapping agent-signal amplifier modified micromotors for capturing based motion and signal amplification strategy. Reproduced from ref. 117 with permission of Elsevier, Copyright 2022.

action of a magnetic field and tested further through two steps of cyclic voltammetry and differential pulse voltammetry. This provides information on the amount of antigen in solution, resulting in higher sensitivity and accuracy than previous MNMs that only enhance convection and mass transfer in electrochemical testing.[116]

The properties of MNMs are continually explored with the aim of improving their performance in electrochemical sensing. As demonstrated in Fig. 6d, Mao *et al.* have coated iron tetroxide nanoparticles with polydopamine and functionalized them with heparin, which can adsorb a high amount of biomolecules due to its porous structure. The particles were loaded with magnesium ion-responsive DNA hydrolase, a nucleic acid-specific enzyme that can break down the nucleic acid at specific sites in the presence of magnesium ions. By only functionalizing one side of the magnesium particle (forming a Janus structure), the other side reacted with water to generate bubbles, resulting in the movement of the MNM. When this type of MNM is used for a specific nucleic acid strand detection, the target nucleic acid strand binds specifically to the DNA hydrolase and then splits in the presence of magnesium ions into a marker strand that can be used for testing, which then further binds to the next DNA hydrolase and is cleaved again. Through multiple binding–cleavage cycles, multiple marker strands can be generated from a single target nucleic acid strand, which then binds to a complementary strand with an electrochemically active material to increase the signal intensity. As the magnesium particles are consumed by the reaction, the iron tetroxide particles are released and can then be attracted to the electrode surface by a magnetic field and ultimately detected.[117] This approach significantly reduces the detection limits of specific nucleic acid chains through amplification effects and results in a high sensitivity. The same group modified antibodies specific to oxidized low-density lipoprotein (Ox-LDL) onto the surface of magnesium (Mg)–Fe_3O_4@Prussian blue micromotors, creating an electrochemical sensor for Ox-LDL.[118] The movement of these micromotors enhances the capture of Ox-LDL, while the catalytic effect of Prussian blue on H_2O_2 reduction enables the determination of current signals. However, the presence of Ox-LDL impedes electron transfer, leading to a decrease in the value of the current signal. These examples highlight the important role that MNMs can play in electrochemical sensing.

The movement of MNMs causes convection in a solution, disrupting the diffusion layer at the electrode surface. Based on this, sensing systems for microbial detection have been created. A detection device for *E. coli* has been developed, in which the presence of the bacteria affects the diffusion of hydroxyl groups to the electrode surface. This, in turn, affects the strength of the electrode's detection signal, allowing for the determination of the concentration of *E. coli*.[119] In addition to the sensing applications of MNMs described above, electrochemical sensing methods are also important in the study of the propulsion mechanism of MNMs.

In recent years, electrochemical sensing using MNMs has emerged as a popular research direction in the field of sensing, due to its high sensitivity and reliability compared to other detection methods. The simple testing equipment and relatively low cost make it an attractive choice. However, the general lack of selectivity in electrochemical testing methods requires specialized structural designs for MNMs, which presents a challenge in their development and limits their use in complex liquid environments.

3.4 Intelligent sensing of MNMs based on other methods

In addition to the aforementioned combination of optical and electrochemical detection methods based on the motion behavior of the MNMs, there are various other detection methods that have also been employed for MNM smart sensing. As shown in Fig. 7a, the magnetically driven nanorods that

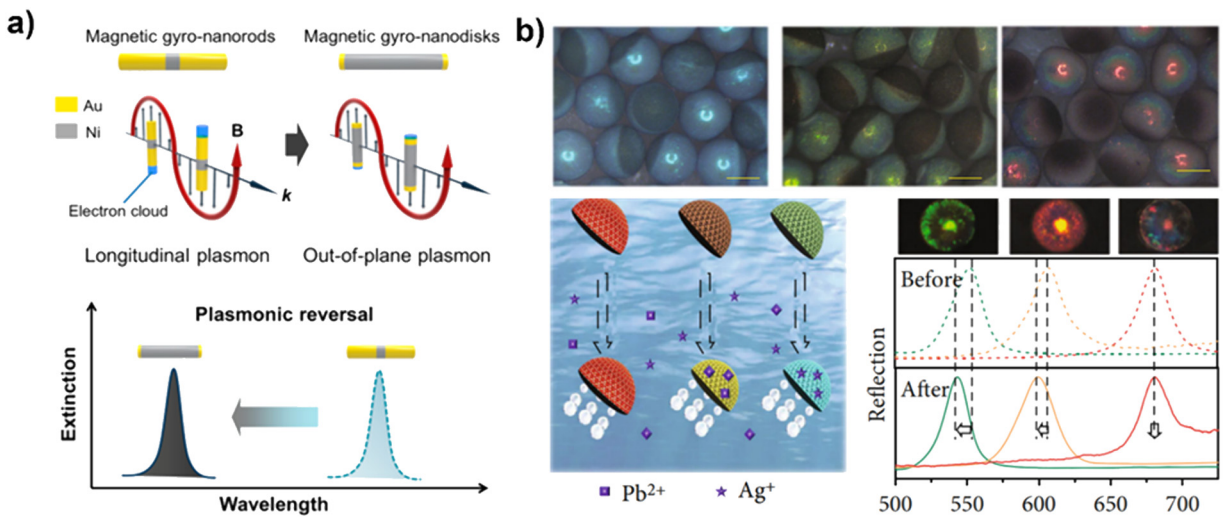

Fig. 7 Sensing using MNMs based on other methods. (a) The change of periodic extinction signal based on antigen–antibody binding. Reprinted from ref. 120 with permission of the American Chemical Society, copyright 2018. (b) The structural color of MNM for sensing specific ions. Reproduced from ref. 121 with permission of American Association for the Advancement of Science, Copyright 2021.

can achieve rotational motion under a rotating magnetic field have been prepared. Due to the anisotropic nature of the nanorod, collective fluctuations in the surface plasma occur during rotation, resulting in a periodic extinction signal that can be output as a frequency signal *via* Fourier transform. After the antigen is captured, the measured frequency signal decreases due to changes in the surface structure. Based on this relationship between frequency changes and antigen concentration, intelligent sensing devices can be fabricated.[120]

The spectral properties of materials can change due to alterations in their chemical molecular structure. Additionally, some materials with structural coloration can also be used in combination with MNMs for colorimetric sensing. Structural colors are produced by the systematic arrangement of a material's microstructure and can be analyzed both optically, using a microscope, and spectroscopically for precise quantification. To realize multiplex label-free detection, Zhao *et al.*[121] created Janus-structured color microspheres consisting of graphene oxide and inverse opal on each side, through phase separation of graphene oxide and silica nanoparticles in a mixed solution using a microfluidic device, as demonstrated in Fig. 7b. The structural color MNM, created through the pre-mixing of graphene oxide, platinum nanoparticles, and ferric oxide particles, has a unique ability to move in both bubble-driven and magnetic field-driven modes in a hydrogen peroxide solution. Its surface is coated with a hydrogel containing an aptamer that can bind to specific ions, resulting in a change in structural color. This offers a label-free detection method that utilizes the spectral change of the MNM to indicate the presence or absence of ions, with the amount being quantitatively described by the degree of shift in the spectrum. By modifying aptamers for different ions on different MNMs, it can perform parallel label-free detection of multiple ions. Furthermore, Guan *et al.*[122,123] integrated magnetically driven swarming with structural colors to sense complex environments, which is achieved by accurately mapping local physicochemical conditions, such as pH, temperature, and glucose concentration. In conclusion, the use of structural color MNMs provides a simple, convenient, and sensitive means of multiplex detection through simple spectroscopic tests, making it a promising option for high-throughput testing.

4. Advantages of smart sensing enabled by MNMs

4.1 Enhanced mass transfer by MNM motion in low Reynolds conditions

Efficient and homogeneous fluid mixing is critical for a range of microfluidic applications, including intricate chemical reactions, small molecule analysis, and biochemistry assays. However, fluids at the micro and nano scales typically exhibit laminar flow, characterized by a low Reynolds number (calculated as the ratio of fluid density, flow velocity, characteristic length, and dynamic viscosity of the fluid). In these conditions, mixing of solutions relies primarily on passive diffusion, which is a slow process and results in low detection efficiency, hindering rapid and immediate detection. To enhance the mixing of substances and reduce solution mixing times, various strategies have been explored. These can be broadly classified into two categories: passive and active. Each method has its own advantages and limitations in terms of efficacy, mixing time, control, and ease of use. Passive mixers are simple to operate as they do not require any external equipment or power source and can be integrated with various inspection applications. However, their mixing efficiency is low. On the other hand, active mixing employs external sources such as ultrasound, magnetic fields, electric fields, *etc.* to drive the particles, resulting in more efficient and homogeneous mixing. MNMs exhibit the capability to move in low Reynolds number conditions and intelligent detection probes based on MNMs can be designed to achieve various controlled movement patterns. These probes can generate micro/nano scale perturbations, accelerate the binding of the molecules and quickly reach kinetic equilibrium.

4.2 Precise targeting and controlled detection of the substance at the micro and nano scale

Presently, detection probes predominantly rely on passive diffusion to arrive the detection site, which results in limited control and hinders the ability to precisely target microscopic lesion locations. While the microprobe approach offers the ability to detect specific target locations, it requires a sophisticated control platform and is also destructive to tissue. In contrast, smart detection probes based on MNMs can achieve controlled targeting of measurement sites and offer the potential for dynamic detection with less tissue destruction, making them a promising option for future development of intelligent detection probes.

4.3 Automated detection through controlled detection probes

The use of automated equipment has become increasingly prevalent in the market, primarily utilizing passive probes. However, these passive probes necessitate complex mechanical control systems for automation of the cleaning process and solution transfer, leading to higher instrument costs and hindering the advancement of cost-effective, miniaturized devices for point-of-care testing (POCT). To simplify external operations and reduce costs, smart detection probes based on MNMs offer a promising alternative. These probes can be directly controlled by external magnetic fields, eliminating the need for complex mechanical control systems. With the foundation of MNM motion that can be manipulated, it is possible to operate detection probes directly at the micro-nano scale for automated detection.

4.4 Combining MNMs with smartphones

The integration of MNMs and smartphone technology has paved the way for the development of digital smart clinic systems. For instance, the use of magnetic nanorobots as detection probes by Kristin Weidemaier has made it possible to rapidly diagnose patients with Ebola virus-induced fever.[125]

Bubble-driven MNMs in combination with a mobile phone to enable detection of target substances by analyzing motion changes were fabricated by Harvard Medical School.[126] In the future, the advancement of smartphone microphotographic optics and accompanying detection software could further enhance the rapid detection capabilities of various substances.

5. Limitations and challenges of smart sensing enabled by MNMs

Although the MNMs exhibit great potential as biosensing platforms due to the advantages in the mixing and separation of substances, there are still some limitations and challenges of smart sensing enabled by MNMs (Table 1).

5.1 Influence of reaction substrate on MNM motion and sensing

During the initial phase, MNMs primarily relied on chemical propulsion, with a particular focus on a group of MNMs propelled by the platinum-catalyzed decomposition of hydrogen peroxide, resulting in bubble generation or the formation of ion gradients. When employing a chemically driven MNM for sensing and detection purposes, the addition of substrates to the target object becomes necessary. However, this introduces interference factors into the detection system and consequently adds background noise to the obtained results. Correspondingly, the substances in the analytes, such as proteins and ionic strength, also affect the motion of the MNM propelled by the self-diffusiophoresis and self-electrophoresis. On the other hand, the chemically driven MNMs have a high dependence on the substrate, and the motion changes with the substrate concentration, and the stability is poor.

5.2 Lack of exploration of *in vivo in situ* detection

Currently, the majority of experiments are conducted *in vitro*, and there is a scarcity of genuine exploration experiments for *in vivo in situ* sensing detection.[127,128] *In vivo* testing encounters several challenges, primarily falling into the following categories. Firstly, within the intricate internal environment, the control complexity of MNMs is amplified, leading to an increase in uncertainty factors. Secondly, due to the small size of MNMs, efficiently and rapidly delivering them to larger target positions within the macroscopic human body remains a challenging problem. Finally, the effective transmission of signals between internal MNMs and external components continues to be a challenge. Furthermore, the utilization of micro-nanomaterials (*e.g.*, Pt) and reaction substrates (*e.g.*, hydrogen peroxide) in the construction of chemically driven MNMs poses toxicity concerns for cells and hampers their applications *in vivo* sensing.

5.3 The challenge of detection accuracy and repeatability

Currently, several detection techniques utilizing MNMs have emerged, especially a method that relies on monitoring the alteration in motion of these motors for analyte detection.

Table 1 The propulsion methods, advantages, and limitations of different intelligent sensing

Sensing methods	Propulsion methods	Fuel or energy source	Advantages and limitations	Ref.
Motion change methods	Phoretic propulsion	H_2O_2	Advantages: preparing the setup is straightforward and the detection outcomes are readily observable.	69
	Bubble propulsion	H_2O_2	Limitations: the detection capability is restricted to a single type, and its repeatability is unsatisfactory.	25, 71
	Surface tension gradient propulsion	SDS		72
Colorimetric methods	Magnetic field propulsion	Magnetic field	Advantages: the detection results are widely employed and boast high accuracy.	84
	Bubble propulsion	H_2O_2	Limitations: requiring corresponding professional instruments and the detection principle appears relatively intricate.	86–88
	Light propulsion	Light		89
Fluorescence method	Bubble propulsion	H_2O_2		92, 99, 103, 106
	Magnetic field propulsion	Magnetic field		124
Electrochemiluminescence method	Bubble propulsion	H_2O_2		108
Raman-enhanced spectroscopy method	Light propulsion	Light		109
	Magnetic field propulsion	Magnetic field		110
Electrochemical analysis method	Bubble propulsion	Glucose	Advantages: high sensitivity and reliability	114
	Magnetic field propulsion	Magnetic field	Limitations: lack of selectivity.	116
	Bubble propulsion	H_2O		117
Other methods	Magnetic field propulsion	Magnetic field	Advantages: label-free detection methods	120
	Bubble propulsion	H_2O_2	Limitations: high preparation cost and low yield	121

This method is highly susceptible to environmental influences, leading to a significant increase in the coefficient of variation (CV) value of the test results. Furthermore, the detection limit of this method is constrained and falls short of the detection limits achieved by traditional spectral detection methods. Additionally, both the motion-based detection method and the surface luminescence-based detection method of micro-nanomotors can solely detect a singular analyte, thereby limiting the acquisition of diverse detection information simultaneously.

6. Conclusions

In recent decades, significant resources have been invested in the development of artificial MNMs, aiming to create intelligent platforms capable of efficiently carrying out a wide range of tasks. As compared with passive particles, the tiny MNMs are highly advantageous for use as detection probes due to their tiny size at the micro/nanoscale and high surface area to volume ratio, which allows for efficient adsorption and specific binding. Through biofunctionalization of surface materials, MNMs can be prepared as dynamic micro-biosensors for the rapid and highly sensitive detection of biomolecules (*e.g.*, nucleic acids and proteins) in real time. Additionally, the autonomous movement and precise manipulation capabilities of MNMs facilitate efficient fluid mixing and enhance the binding efficiency of target to the probe. They offer several advantages over traditional sensing methods, including high sensitivity, rapid response time, and the ability to perform multiple sensing functions simultaneously. Despite their potential, the field of MNMs for sensing is still in its early stages and there are several challenges that must be addressed before they can be widely used. As discussed in Section 5, the majority of MNMs are fuel-based, which will not only impact the inherent characteristics of the sensing environment, but also restricts the movement of the MNMs to a brief duration. The external field-driven MNMs present a favorable option for sensing applications. Additionally, MNMs face challenges related to the absence of *in situ* detection tests and the biocompatibility of materials. In the future, it is crucial to enhance the biocompatibility of materials to fabricate MNMs and explore more effective biocompatible propulsion mechanism, such as enzyme-driven and magnetic field-driven approaches. Finally, there is no work which thoroughly addressed the resolution and sensing accuracy of the micromotors in a meticulous manner, despite numerous groups have evaluated the performance of micromotors in selective target detection. Hence, the future sensor detection department based on MNMs should expand beyond *in vitro* simulation detection and include direct real sample detection. In the future, *in situ* detection of MNMs *in vivo* is an important research direction. This requires us to develop higher resolution imaging and *in vivo* tracking techniques. At the same time, we need to improve the materials' structure design and driving methods of MNMs.

Despite the numerous challenges and obstacles, the emerging field of MNMs based platforms has managed to introduce novelty and revolutionize the field of sensing. Early diagnosis can reduce mortality rates and faster and expedite treatment processes, thereby alleviating the burden of high costs. Furthermore, by integrating these MNMs into POCT (Point-of-Care Testing), early disease detection will be facilitated, enabling the monitoring of chronic diseases at an early stage. This comprehensive review may inspire researchers and provide valuable insights, guiding them on the path of exploration and development of intelligent sensing based on MNMs.

Author contributions

J. G., X. M. and Y. W conceived the review concept. L. J., X. L. and D. Z carried out the literature search. L. J. and Y. W. drew the schematic and chemical illustrations. L. J., J. G., X. M. and Y. W. wrote and edited the manuscript. All authors have reviewed the final version of the manuscript.

Conflicts of interest

There are no conflicts to declare.

Acknowledgements

The authors acknowledge the financial support from the National Natural Science Foundation of China (52072095, 51802060, and 62122017).

Notes and references

1 S. Pyo, J. Lee, K. Bae, S. Sim and J. Kim, *Adv. Mater.*, 2021, **33**, 2005902.
2 H. Xu, M. Gao, X. Tang, W. Zhang, D. Luo and M. Chen, *Small Methods*, 2020, **4**, 1900506.
3 P. Li, G.-H. Lee, S. Y. Kim, S. Y. Kwon, H.-R. Kim and S. Park, *ACS Nano*, 2021, **15**, 1960–2004.
4 V. S. P. K. S. A. Jayanthi, A. B. Das and U. Saxena, *Biosens. Bioelectron.*, 2017, **91**, 15–23.
5 N. Rohaizad, C. C. Mayorga-Martinez, M. Fojtu, N. M. Latiff and M. Pumera, *Chem. Soc. Rev.*, 2021, **50**, 619–657.
6 F. Peng, Y. Tu and D. A. Wilson, *Chem. Soc. Rev.*, 2017, **46**, 5289–5310.
7 M. Wan, T. Li, H. Chen, C. Mao and J. Shen, *Angew. Chem., Int. Ed.*, 2021, **60**, 13158–13176.
8 M. Safdar, S. U. Khan and J. Janis, *Adv. Mater.*, 2018, **30**, 1703660.
9 S. Sanchez, L. Soler and J. Katuri, *Angew. Chem., Int. Ed.*, 2015, **54**, 1414–1444.
10 K. J. Rao, F. Li, L. Meng, H. Zheng, F. Cai and W. Wang, *Small*, 2015, **11**, 2836–2846.
11 G. Loget and A. Kuhn, *Nat. Commun.*, 2011, **535**, 1–6.
12 L. Xu, F. Mou, H. Gong, M. Luo and J. Guan, *Chem. Soc. Rev.*, 2017, **46**, 6905–6926.
13 K. Villa and M. Pumera, *Chem. Soc. Rev.*, 2019, **48**, 4966–4978.

14 H. Zhou, C. C. Mayorga-Martinez, S. Pane, L. Zhang and M. Pumera, *Chem. Rev.*, 2021, **121**, 4999–5041.
15 Y. Dong, L. Wang, V. Iacovacci, X. Wang, L. Zhang and B. J. Nelson, *Matter*, 2022, **5**, 77–109.
16 J. Parmar, D. Vilela, K. Villa, J. Wang and S. Sanchez, *J. Am. Chem. Soc.*, 2018, **140**, 9317–9331.
17 L. Soler and S. Sanchez, *Nanoscale*, 2014, **6**, 7175–7182.
18 W. Yu, R. Lin, X. He, X. Yang, H. Zhang, C. Hu, R. Liu, Y. Huang, Y. Qin and H. Gao, *Acta Pharm. Sin. B*, 2021, **11**, 2924–2936.
19 R. Lin, W. Yu, X. Chen and H. Gao, *Adv. Healthcare Mater.*, 2021, **10**, 2001212.
20 J. Li, B. E.-F. de Avila, W. Gao, L. Zhang and J. Wang, *Sci. Rob.*, 2017, **2**, eaam6431.
21 M. Pacheco, M. Angel Lopez, B. Jurado-Sanchez and A. Escarpa, *Anal. Bioanal. Chem.*, 2019, **411**, 6561–6573.
22 L. Kong, J. Guan and M. Pumera, *Curr. Opin. Electrochem.*, 2018, **10**, 174–182.
23 R. Maria-Hormigos, B. Jurado-Sanchez and A. Escarpa, *Anal. Bioanal. Chem.*, 2022, **414**, 7035–7049.
24 T. Patino, A. Porchetta, A. Jannasch, A. Llado, T. Stumpp, E. Schaeffer, F. Ricci and S. Sanchez, *Nano Lett.*, 2019, **19**, 3440–3447.
25 J. Orozco, V. Garcia-Gradilla, M. D'Agostino, W. Gao, A. Cortes and J. Wang, *ACS Nano*, 2013, **7**, 818–824.
26 D. Vilela, J. Parmar, Y. Zeng, Y. Zhao and S. Sánchez, *Nano Lett.*, 2016, **16**, 2860–2866.
27 E. Morales-Narvaez, M. Guix, M. Medina-Sanchez, C. C. Mayorga-Martinez and A. Merkoci, *Small*, 2014, **10**, 2542–2548.
28 M. S. Draz, N. K. Lakshminaraasimulu, S. Krishnakumar, D. Battalapalli, A. Vasan, M. K. Kanakasabaathy, A. Sreeram, S. Kallakuri, P. Thirumalaraju, Y. Li, S. Hua, X. G. Yu, D. R. Kuritzkes and H. Shafiee, *ACS Nano*, 2018, **12**, 5709–5718.
29 C. C. Mayorga-Martinez and M. Pumera, *Adv. Funct. Mater.*, 2020, **30**, 1906449.
30 L. Wang, X. Hao, Z. Gao, Z. Yang, Y. Long, M. Luo and J. Guan, *Interdisciplinary Mater.*, 2022, **1**, 256–280.
31 M. Yang, X. Guo, F. Mou and J. Guan, *Chem. Rev.*, 2023, **123**, 3944–3975.
32 S. Karadkar, A. Tiwari and A. C. Chaskar, *Int. Nano Lett.*, 2023, **13**, 93–115.
33 L. Cai, D. Xu, Z. Zhang, N. Li and Y. Zhao, *Research*, 2023, **6**, 0044.
34 S. K. Panda, N. A. Kherani, S. Debata and D. P. Singh, *Mater. Adv.*, 2023, **4**, 1460–1480.
35 M. N. Popescu and S. Gaspar, *Biosensors*, 2023, **13**, 45.
36 S. H. Chang, *Mater. Today Sustainability*, 2022, **19**, 100196.
37 Y. Hu, W. Liu and Y. Sun, *Adv. Funct. Mater.*, 2022, **32**, 2109181.
38 N. Hirokawa, Y. Noda, Y. Tanaka and S. Niwa, *Nat. Rev. Mol. Cell Biol.*, 2009, **10**, 682–696.
39 L. M. Stabryla, K. A. Johnston, N. A. Diemler, V. S. Cooper, J. E. Millstone, S.-J. Haig and L. M. Gilbertson, *Nat. Nanotechnol.*, 2021, **16**, 996–1003.
40 M. Medina-Sanchez, L. Schwarz, A. K. Meyer, F. Hebenstreit and O. G. Schmidt, *Nano Lett.*, 2016, **16**, 555–561.
41 M. Luo, Y. Feng, T. Wang and J. Guan, *Adv. Funct. Mater.*, 2018, **28**, 1706100.
42 Y. Mei, A. A. Solovev, S. Sanchez and O. G. Schmidt, *Chem. Soc. Rev.*, 2011, **40**, 2109–2119.
43 C. Zhou, C. Gao, Z. Lin, D. Wang, Y. Li, Y. Yuan, B. Zhu and Q. He, *Langmuir*, 2020, **36**, 7039–7045.
44 S. Wang, J. Xu, Q. Zhou, P. Geng, B. Wang, Y. Zhou, K. Liu, F. Peng and Y. Tu, *Adv. Healthcare Mater.*, 2021, **10**, 2100335.
45 S. Gao, J. Hou, J. Zeng, J. J. Richardson, Z. Gu, X. Gao, D. Li, M. Gao, D.-W. Wang, P. Chen, V. Chen, K. Liang, D. Zhao and B. Kong, *Adv. Funct. Mater.*, 2019, **29**, 1808900.
46 L. Zhao, Y. Liu, S. Xie, P. Ran, J. Wei, Q. Liu and X. Li, *Chem. Eng. J.*, 2020, **382**, 123041.
47 J. Wang, Z. Xiong, X. Zhan, B. Dai, J. Zheng, J. Liu and J. Tang, *Adv. Mater.*, 2017, **29**, 1701451.
48 R. Liu and A. Sen, *J. Am. Chem. Soc.*, 2011, **133**, 20064–20067.
49 W. F. Paxton, A. Sen and T. E. Mallouk, *Chem. – Eur. J.*, 2005, **11**, 6462–6470.
50 M. Yan, T. Liu, X. Li, S. Zhou, H. Zeng, Q. Liang, K. Liang, X. Wei, J. Wang, Z. Gu, L. Jiang, D. Zhao and B. Kong, *J. Am. Chem. Soc.*, 2022, **144**, 7778–7789.
51 S.-Y. Tang, V. Sivan, K. Khoshmanesh, A. P. O'Mullane, X. Tang, B. Gol, N. Eshtiaghi, F. Lieder, P. Petersen, A. Mitchell and K. Kalantar-zadeh, *Nanoscale*, 2013, **5**, 5949–5957.
52 D. Jin, J. Yu, K. Yuan and L. Zhang, *ACS Nano*, 2019, **13**, 5999–6007.
53 T. O. Tasci, P. S. Herson, K. B. Neeves and D. W. M. Marr, *Nat. Commun.*, 2016, **7**, 10225.
54 X. Wang, X.-H. Qin, C. Hu, A. Terzopoulou, X.-Z. Chen, T.-Y. Huang, K. Maniura-Weber, S. Pané and B. J. Nelson, *Adv. Funct. Mater.*, 2018, **28**, 1804107.
55 D. Walker, B. T. Käsdorf, H.-H. Jeong, O. Lieleg and P. Fischer, *Sci. Adv.*, 2015, **1**, e1500501.
56 W. Hu, G. Z. Lum, M. Mastrangeli and M. Sitti, *Nature*, 2018, **554**, 81–85.
57 H. Xie, M. Sun, X. Fan, Z. Lin, W. Chen, L. Wang, L. Dong and Q. He, *Sci. Rob.*, 2019, **4**, eaav8006.
58 J. Guo, J. J. Gallegos, A. R. Tom and D. Fan, *ACS Nano*, 2018, **12**, 1179–1187.
59 W. Wang, L. A. Castro, M. Hoyos and T. E. Mallouk, *ACS Nano*, 2012, **6**, 6122–6132.
60 T. Xu, F. Soto, W. Gao, V. Garcia-Gradilla, J. Li, X. Zhang and J. Wang, *J. Am. Chem. Soc.*, 2014, **136**, 8552–8555.
61 Q. Zhang, R. Dong, Y. Wu, W. Gao, Z. He and B. Ren, *ACS Appl. Mater. Interfaces*, 2017, **9**, 4674–4683.
62 R. Dong, Q. Zhang, W. Gao, A. Pei and B. Ren, *ACS Nano*, 2016, **10**, 839–844.
63 Y. Wu, T. Si, J. Shao, Z. Wu and Q. He, *Nano Res.*, 2016, **9**, 3747–3756.
64 R. Dong, Y. Hu, Y. Wu, W. Gao, B. Ren, Q. Wang and Y. Cai, *J. Am. Chem. Soc.*, 2017, **139**, 1722–1725.

65 L. Liu, S. Li, K. Yang, Z. Chen, Q. Li, L. Zheng, Z. Wu, X. Zhang, L. Su, Y. Wu and J. Song, *Nano Lett.*, 2023, **23**, 3929–3938.
66 H. Xu, M. Medina-Sánchez, V. Magdanz, L. Schwarz, F. Hebenstreit and O. G. Schmidt, *ACS Nano*, 2018, **12**, 327–337.
67 R. Maria-Hormigos, C. C. Mayorga-Martinez, T. Kinčl and M. Pumera, *ACS Nano*, 2023, **17**, 7595–7603.
68 D. Luo, A. Maheshwari, A. Danielescu, J. Li, Y. Yang, Y. Tao, L. Sun, D. K. Patel, G. Wang, S. Yang, T. Zhang and L. Yao, *Nature*, 2023, **614**, 463–470.
69 D. Kagan, P. Calvo-Marzal, S. Balasubramanian, S. Sattayasamitsathit, K. M. Manesh, G.-U. Flechsig and J. Wang, *J. Am. Chem. Soc.*, 2009, **131**, 12082–12083.
70 D. Zhang, D. Wang, J. Li, X. Xu, H. Zhang, R. Duan, B. Song, D. Zhang and B. Dong, *J. Mater. Sci.*, 2019, **54**, 7322–7332.
71 Y. Su, Y. Ge, L. Liu, L. Zhang, M. Liu, Y. Sun, H. Zhang and B. Dong, *ACS Appl. Mater. Interfaces*, 2016, **8**, 4250–4257.
72 L. Liu, Y. Dong, Y. Sun, M. Liu, Y. Su, H. Zhang and B. Dong, *Nano Res.*, 2016, **9**, 1310–1318.
73 G. Zhao, S. Sanchez, O. G. Schmidt and M. Pumera, *Nanoscale*, 2013, **5**, 2909–2914.
74 V. V. Singh, K. Kaufmann, B. E.-F. de Avila, M. Uygun and J. Wang, *Chem. Commun.*, 2016, **52**, 3360–3363.
75 I. Ortiz-Rivera, T. M. Courtney and A. Sen, *Adv. Funct. Mater.*, 2016, **26**, 2135–2142.
76 K. Van Nguyen and S. D. Minteer, *Chem. Commun.*, 2015, **51**, 4782–4784.
77 S. Fu, X. Zhang, Y. Xie, J. Wu and H. Ju, *Nanoscale*, 2017, **9**, 9026–9033.
78 Y. Xie, S. Fu, J. Wu, J. Lei and H. Ju, *Biosens. Bioelectron.*, 2017, **87**, 31–37.
79 X. Zhang, C. Chen, J. Wu and H. Ju, *ACS Appl. Mater. Interfaces*, 2019, **11**, 13581–13588.
80 T. Patino, A. Porchetta, A. Jannasch, A. Lladó, T. Stumpp, E. Schäffer, F. Ricci and S. Sánchez, *Nano Lett.*, 2019, **19**, 3440–3447.
81 M. S. Draz, K. M. Kochehbyoki, A. Vasan, D. Battalapalli, A. Sreeram, M. K. Kanakasabapathy, S. Kallakuri, A. Tsibris, D. R. Kuritzkes and H. Shafiee, *Nat. Commun.*, 2018, **9**, 4282.
82 K. Yuan, C. Cuntín-Abal, B. Jurado-Sánchez and A. Escarpa, *Anal. Chem.*, 2021, **93**, 16385–16392.
83 G. C. Cogal, G. Y. Karaca, E. Uygun, F. Kuralay, L. Oksuz, M. Remskar and A. U. Oksuz, *Anal. Chim. Acta*, 2020, **1138**, 69–78.
84 Y. Wang, X. Liu, C. Chen, Y. Chen, Y. Li, H. Ye, B. Wang, H. Chen, J. Guo and X. Ma, *ACS Nano*, 2022, **16**, 180–191.
85 B. E.-F. de Ávila, M. Zhao, S. Campuzano, F. Ricci, J. M. Pingarrón, M. Mascini and J. Wang, *Talanta*, 2017, **167**, 651–657.
86 R. María-Hormigos, B. Jurado-Sánchez and A. Escarpa, *Anal. Chem.*, 2018, **90**, 9830–9837.
87 R. María-Hormigos, Á. Molinero-Fernández, M. Á. López, B. Jurado-Sánchez and A. Escarpa, *Anal. Chem.*, 2022, **94**, 5575–5582.
88 B. Jurado-Sánchez, J. Wang and A. Escarpa, *ACS Appl. Mater. Interfaces*, 2016, **8**, 19618–19625.
89 M. Palacios-Corella, D. Rojas and M. Pumera, *J. Colloid Interface Sci.*, 2023, **631**, 125–134.
90 B. Jurado-Sánchez, A. Escarpa and J. Wang, *Chem. Commun.*, 2015, **51**, 14088–14091.
91 T. Li, Y. Lyu, J. Li, C. Wang, N. Xing, J. Yang and M. Zuo, *Environ. Sci.: Nano*, 2021, **8**, 3833–3845.
92 V. V. Singh, K. Kaufmann, J. Orozco, J. Li, M. Galarnyk, G. Arya and J. Wang, *Chem. Commun.*, 2015, **51**, 11190–11193.
93 M. Pacheco, B. Jurado-Sánchez and A. Escarpa, *Anal. Chem.*, 2018, **90**, 2912–2917.
94 K. Wang, E. Ma, Z. Hu and H. Wang, *Chem. Commun.*, 2021, **57**, 10528–10531.
95 Y. Yuan, C. Gao, D. Wang, C. Zhou, B. Zhu and Q. He, *Beilstein J. Nanotechnol.*, 2019, **10**, 1324–1331.
96 M. Liu, Y. Sun, T. Wang, Z. Ye, H. Zhang, B. Dong and C. Y. Li, *J. Mater. Chem. C*, 2016, **4**, 5945–5952.
97 W. Yang, J. Li, Z. Xu, J. Yang, Y. Liu and L. Liu, *J. Mater. Chem. C*, 2019, **7**, 10297–10308.
98 Q. Wang, T. Li, D. Fang, X. Li, L. Fang, X. Wang, C. Mao, F. Wang and M. Wan, *Microchem. J.*, 2020, **158**, 105125.
99 Á. Molinero-Fernández, M. Moreno-Guzmán, M. Á. López and A. Escarpa, *Anal. Chem.*, 2017, **89**, 10850–10857.
100 K. Yuan, M. Á. López, B. Jurado-Sánchez and A. Escarpa, *ACS Appl. Mater. Interfaces*, 2020, **12**, 46588–46597.
101 B. E.-F. de Avila, M. A. Lopez-Ramirez, D. F. Baez, A. Jodra, V. V. Singh, K. Kaufmann and J. Wang, *ACS Sens.*, 2016, **1**, 217–221.
102 J. Gordón, L. Arruza, M. D. Ibáñez, M. Moreno-Guzmán, M. Á. López and A. Escarpa, *ACS Sens.*, 2022, **7**, 3144–3152.
103 M. Pacheco, V. D. L. Asunción-Nadal, B. Jurado-Sánchez and A. Escarpa, *Biosens. Bioelectron.*, 2020, **165**, 112286.
104 V. D. la Asunción-Nadal, M. Pacheco, B. Jurado-Sánchez and A. Escarpa, *Anal. Chem.*, 2020, **92**, 9188–9193.
105 K. Yuan, V. de la Asunción-Nadal, C. Cuntín-Abal, B. Jurado-Sánchez and A. Escarpa, *Lab Chip*, 2022, **22**, 928–935.
106 Á. Molinero-Fernández, M. Moreno-Guzmán, L. Arruza, M. Á. López and A. Escarpa, *ACS Sens.*, 2020, **5**, 1336–1344.
107 L. Cai, H. Wang, Y. Yu, F. Bian, Y. Wang, K. Shi, F. Ye and Y. Zhao, *Natl. Sci. Rev.*, 2019, **7**, 644–651.
108 M. Sentic, S. Arbault, B. Goudeau, D. Manojlovic, A. Kuhn, L. Bouffier and N. Sojic, *Chem. Commun.*, 2014, **50**, 10202–10205.
109 Y. Wang, C. Zhou, W. Wang, D. Xu, F. Zeng, C. Zhan, J. Gu, M. Li, W. Zhao, J. Zhang, J. Guo, H. Feng and X. Ma, *Angew. Chem., Int. Ed.*, 2018, **57**, 13110–13113.
110 Y. Wang, Y. Liu, Y. Li, D. Xu, X. Pan, Y. Chen, D. Zhou, B. Wang, H. Feng and X. Ma, *Research*, 2020, **2020**, 1–13.
111 X. Fan, Q. Hao, M. Li, X. Zhang, X. Yang, Y. Mei and T. Qiu, *ACS Appl. Mater. Interfaces*, 2020, **12**, 28783–28791.
112 X. Liu, W. Chen, D. Zhao, X. Liu, Y. Wang, Y. Chen and X. Ma, *ACS Nano*, 2022, **16**, 10354–10363.
113 A. L. Furst and M. B. Francis, *Chem. Rev.*, 2019, **119**, 700–726.
114 L. Kong, N. Rohaizad, M. Z. M. Nasir, J. Guan and M. Pumera, *Anal. Chem.*, 2019, **91**, 5660–5666.

115 D. Rojas, B. Jurado-Sánchez and A. Escarpa, *Anal. Chem.*, 2016, **88**, 4153–4160.
116 E. Ma, K. Wang and H. Wang, *Microchim. Acta*, 2022, **189**, 47.
117 Q. Wang, X. Tang, R. Lv, K. Tan, Z. Zhao, M. Wan and C. Mao, *Chem. Eng. J.*, 2022, **430**, 132665.
118 D. Fang, S. Tang, Z. Wu, C. Chen, M. Wan, C. Mao and M. Zhou, *Biosens. Bioelectron.*, 2022, **217**, 114682.
119 A. Ramanujam, B. Neyhouse, R. A. Keogh, M. Muthuvel, R. K. Carroll and G. G. Botte, *Chem. Eng. J.*, 2021, **411**, 128453.
120 I. Jung, S. Ih, H. Yoo, S. Hong and S. Park, *Nano Lett.*, 2018, **18**, 1984–1992.
121 H. Wang, L. Cai, D. Zhang, L. Shang and Y. Zhao, *Research*, 2021, **2021**, 1–12.
122 L. Li, Z. Yu, J. Liu, M. Yang, G. Shi, Z. Feng, W. Luo, H. Ma, J. Guan and F. Mou, *Nano-Micro Lett.*, 2023, **15**, 141.
123 Z. Yu, L. Li, F. Mou, S. Yu, D. Zhang, M. Yang, Q. Zhao, H. Ma, W. Luo, T. Li and J. Guan, *InfoMat*, 2023, e12464.
124 Y. Zhang, L. Zhang, L. Yang, C. I. Vong, K. F. Chan, W. K. K. Wu, T. N. Y. Kwong, N. W. S. Lo, M. Ip, S. H. Wong, J. J. Y. Sung, P. W. Y. Chiu and L. Zhang, *Sci. Adv.*, 2019, **5**, eaau9650.
125 M. S. Draz, N. K. Lakshminaraasimulu, S. Krishnakumar, D. Battalapalli, A. Vasan, M. K. Kanakasabapathy, A. Sreeram, S. Kallakuri, P. Thirumalaraju, Y. Li, S. Hua, X. G. Yu, D. R. Kuritzkes and H. Shafiee, *ACS Nano*, 2018, **12**, 5709–5718.
126 M. S. Draz, A. Vasan, A. Muthupandian, M. K. Kanakasabapathy, P. Thirumalaraju, A. Sreeram, S. Krishnakumar, V. Yogesh, W. Lin, X. G. Yu, R. T. Chung and H. Shafiee, *Sci. Adv.*, 2020, **6**, eabd5354.
127 A. C. Hortelao, C. Simó, M. Guix, S. Guallar-Garrido, E. Julián, D. Vilela, L. Rejc, P. Ramos-Cabrer, U. Cossío, V. Gómez-Vallejo, T. Patiño, J. Llop and S. Sánchez, *Sci. Rob.*, 2021, **6**, eabd2823.
128 D. Xu, J. Hu, X. Pan, S. Sánchez, X. Yan and X. Ma, *ACS Nano*, 2021, **15**, 11543–11554.